The Journal of Organic Chemistry

Supporting Information

π-Extended Thiadiazoles Fused with Thienopyrrole or Indole Moieties: Synthesis, Structures, and Properties

Shin-ichiro Kato,[a] Takayuki Furuya,[a] Atsushi Kobayashi,[a] Masashi Nitani,[b] Yutaka Ie,[b,c] Yoshio Aso,[b] Toshitada Yoshihara,[a] Seiji Tobita,[a] and Yosuke Nakamura*[a]

[a] *Department of Chemistry and Chemical Biology, Graduate School of Engineering, Gunma University, 1-5-1, Tenjin-cho, Kiryu, Gunma 376-8515, Japan,* [b] *The Institute of Scientific and Industrial Research (ISIR), Osaka University, 8-1, Mihogaoka, Ibaraki, Osaka 567-0047, Japan,* [c] *PRESTO-JST, 4-1-8 Honcho, Kawaguchi, Saitama 333-0012, Japan*

E-mail: nakamura@gunma-u.ac.jp

Tel: +81-277-30-1310

Fax: +81-277-30-1314

Table of Contents

1. General Experimental Methods

THF was freshly distilled from sodium and benzophenone under argon atmosphere. Column chromatography and plug filtrations were carried out with SiO_2. Thin-layer chromatography (TLC) was conducted on aluminum sheets coated with SiO_2; visualization with a lamp (254 or 365 nm). Melting points (M.p.) are uncorrected. ^{1}H NMR spectra were determined in $CDCl_3$ at 298 K. Residual solvent signals in the ^{1}H and ^{13}C NMR spectra were used as an internal reference. Chemical shifts (δ) are given as δ values. The coupling constants (J) are given in Hz. The apparent resonance multiplicity is described as s (singlet), d (doublet), t (triplet), q (quartet), and m (multiplet). FAB-MS spectra were recorded with *m*-nitrobenzyl alcohol (NBA) as a matrix. MALDI-TOF-MS spectra were recorded with dithranol (Dith) as a matrix. The most important signals are reported in *m*/*z* units with *M* as the molecular ion. UV–vis spectra and fluorescence spectra were measured in a cuvette of 1 cm at 298 K. The absorption maxima (λ_{max}) are reported in nm with the relative intensity or the molar absorptivity in brackets. Shoulders are indicated as sh. Compounds **6**,[1] **7**,[2] and **9**[3] were prepared according to the literature procedures. Cyclic voltammetry was performed by using a cell equipped with a platinum as working electrode, a platinum wire as counter electrodes, and $Ag/AgNO_3$ as the referential electrode. All electrochemical measurements were performed in *o*-DCB solution (*ca.* 5×10^{-4} M) containing 0.1 M *n*-Bu_4NPF_6 at 298 K. All potentials are referenced to the ferrocenium/ferrocene (Fc^+/Fc) couple, used as a standard. Theoretical calculations were performed using the Gaussian 03 program package.[3] Molecular properties in the electronic ground state were computed using the hybrid B3LYP DFT method.[4] Geometry optimization of **1b**–**5b** was performed with no symmetry constrains at the 6-31G* basis set.[5] Frequency calculations on these optimized geometries revealed no imaginary frequencies. Further single-point calculations were performed at the 6-311G** basis set[6] to obtain the molecular orbital energies with use of optimized structures at the B3LYP/6-31G* level of theory. TD calculations for **1b**–**5b** were performed at the B3LYP/6-31G* level of theory with use of optimized structures at the B3LYP/6-31G* level of theory. The calculated UV/Vis transitions are vertical.

2. X-ray Data for Compounds 1a, 1b, 2b, 4a, and 5b

The X-ray crystal structures were solved by direct methods (SIR-97)[7] and refined by full-matrix least-squares analysis (SHELXL-97),[8] using an isotropic extinction correction. All non-hydrogen atoms were refined anisotropically; hydrogen atoms were refined isotropically, whereby hydrogen positions are based on stereochemical considerations. CCDC-879807 (**1a**), CCDC-879808 (**1b**), CCDC-879809 (**2b**), CCDC-879810 (**4a**), and CCDC-879811 (**5b**) contain the supplementary crystallographic data (excluding structure factors) for this paper. These data can be obtained free of charge from The Cambridge Crystallographic Data Centre, 12 Union Road, Cambridge CB2 1EZ, UK (fax: +44(1223)-336-033; e-mail: deposit@ccdc.cam.ac.uk), or via www.ccdc.cam.ac. Uk/data _request/cif

*X-ray crystal structure of **1a***: Crystal data at 173 K for $C_{14}H_6N_4S_3 \cdot H_2O$, M_r = 342.41, Monoclinic, space group $P2_1/n$, D_{calcd} = 1.665 g cm^{-3}, Z = 4, a = 7.744(8) Å, b = 17.07(2) Å, c = 10.665(11) Å, β = 104.32(2)°, V = 1366(3) Å^3; Mo-$K\alpha$ radiation, λ = 0.71075, μ = 0.548 mm^{-1}. A yellow crystal (linear dimensions ca. 0.08 × 0.05 × 0.01 mm) was obtained from acetone/hexane solution at –15 °C. Numbers of measured and unique reflections were 10772 and 2380, respectively (R_{int} = 0.069). Final $R(F)$ = 0.060, $wR(F^2)$ = 0.158 for 205 parameters and 2380 reflections with $I > 2\sigma(I)$ and 2.75 < θ < 24.71° (corresponding R values based are 0.075 and 0.184, respectively, for all data).

*X-ray crystal structure of **1b***: Crystal data at 123 K for $C_{18}H_{14}N_4S_3$, M_r = 382.51, Monoclinic, space group $C2/c$, D_{calcd} = 1.511 g cm^{-3}, Z = 4, a = 13.891(3) Å, b = 11.994(3) Å, c = 12.028(3) Å, β = 122.982(2)°, V = 1680.9(7) Å^3; Mo-$K\alpha$ radiation, λ = 0.71070, μ = 0.450 mm^{-1}. A yellow crystal (linear dimensions ca. 0.50 × 0.50 × 0.45 mm) was obtained from CH_2Cl_2/hexane solution at –15 °C. Numbers of measured and unique reflections were 3684 and 1415, respectively (R_{int} = 0.022). Final $R(F)$ = 0.038, $wR(F^2)$ = 0.100 for 115 parameters and 1415 reflections with $I > 2\sigma(I)$ and 5.41° < θ < 25.00° (corresponding R values based are 0.039 and 0.101, respectively, for all data).

*X-ray crystal structure of **2b***: Crystal data at 150 K for $C_{18}H_{14}N_4S_3$, M_r = 382.51, Monoclinic,

space group $P2_1/n$, D_{calcd} = 1.508 g cm^{-3}, Z = 4, a = 7.961(3) Å, b = 9.065(4) Å, c = 23.363(8) Å, β = 92.484(4)°, V = 1684.4(11) Å^3; Mo-$K\alpha$ radiation, λ = 0.71070, μ = 0.449 mm^{-1}. A yellow crystal (linear dimensions ca. 0.20 × 0.20 × 0.15 mm) was obtained from CH_2Cl_2/hexane solution at –15 °C. Numbers of measured and unique reflections were 7246 and 2868, respectively (R_{int} = 0.028). Final $R(F)$ = 0.044, $wR(F^2)$ = 0.147 for 228 parameters and 2868 reflections with $I > 2\sigma(I)$ and 5.93 < θ < 25.00° (corresponding R values based are 0.047 and 0.152, respectively, for all data).

X-ray crystal structure of ***4a***: Crystal data at 123 K for $C_{26}H_{26}N_4S \cdot H_2O$, M_r = 442.57, Orthorhombic, space group *Fdd*2, D_{calcd} = 1.282 g cm^{-3}, Z = 16, a = 19.399(3) Å, b = 73.053(6) Å, c = 6.4702(7) Å, V = 9169.6(18) Å^3; Mo-$K\alpha$ radiation, λ = 0.71070, μ = 0.167 mm^{-1}. A pale green crystal (linear dimensions ca. 0.40 × 0.35 × 0.30 mm) was obtained from acetone/hexane solution at –15 °C. Numbers of measured and unique reflections were 7654 and 3687, respectively (R_{int} = 0.024). Final $R(F)$ = 0.035, $wR(F^2)$ = 0.010 for 296 parameters and 3687 reflections with $I > 2\sigma(I)$ and 5.34 < θ < 24.99° (corresponding R values based are 0.035 and 0.104, respectively, for all data).

X-ray crystal structure of ***5b***: Crystal data at 173 K for $C_{24}H_{22}N_4O_2S$, M_r = 430.52, Orthorhombic, space group $Pna2_1$, D_{calcd} = 1.444 g cm^{-3}, Z = 4, a = 21.1724(11) Å, b = 13.2827(5) Å, c = 7.0396(2) Å, V = 1979.72(14) Å^3; Mo-$K\alpha$ radiation, λ = 0.71070, μ = 0.195 mm^{-1}. A pale yellow crystal (linear dimensions ca. 0.40 × 0.30 × 0.10 mm) was obtained from CH_2Cl_2/hexane solution at –15 °C. Numbers of measured and unique reflections were 9531 and 3230, respectively (R_{int} = 0.012). Final $R(F)$ = 0.026, $wR(F^2)$ = 0.071 for 284 parameters and 3230 reflections with $I > 2\sigma(I)$ and 5.44 < θ < 24.99° (corresponding R values based are 0.026 and 0.071, respectively, for all data).

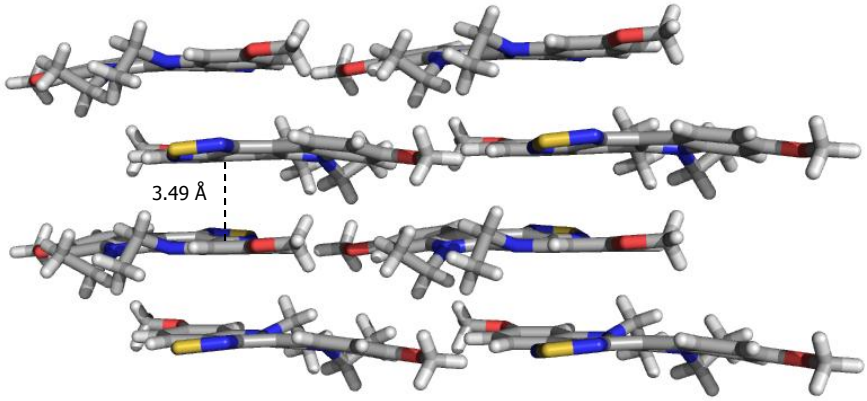

Figure S1. Packing of **5b** in the crystalline state. View perpendicular to the *b,c* plane. The offset stacking leads to a brickwork motif.

3. UV–vis and Fluorescence Data

Table S1. Summary of Photophysical Data of **1a**–**1c**

	solv.	λ_{max} [nm (eV)]	λ_{em} [nm]	τ_f [ns][a]	Φ_f	k_r [10^7 s^{-1}][b]	k_{nr} [10^7 s^{-1}][c]
1a	toluene	420 (2.95)	509	19.1	0.68	3.6	1.7
	THF	424 (2.92)	525	22.6	0.50	2.2	2.2
	EtOAc	421 (2.94)	523	23.0	0.51	2.2	2.1
	CH_2Cl_2	423 (2.93)	549	14.4	0.25	1.7	5.2
	DMF	432 (2.86)	563	18.9	0.30	1.6	3.7
1b	toluene	432 (2.91)	523	19.4	0.73	3.8	1.4
	THF	436 (2.85)	539	23.7	0.68	2.9	1.4
	EtOAc	433 (2.87)	538	24.2	0.63	2.6	1.5
	CH_2Cl_2	436 (2.85)	565	16.6	0.33	2.0	4.0
	DMF	441 (2.82)	573	22.1	0.42	1.9	2.6
1c	toluene	432 (2.86)	522	19.1	0.73	3.8	1.4
	CH_2Cl_2	434 (2.85)	559	19.4	0.39	2.0	3.1

[a] Lifetime. [b] Radiative constant. [c] Non-radiative constant.

Table S2. Summary of Photophysical Data of **2a**–**2c**

	solv.	λ_{max} [nm (eV)]	λ_{em} [nm]	τ_f [ns][a]	Φ_f	k_r [10^7 s^{-1}][b]	k_{nr} [10^7 s^{-1}][c]
2a	toluene	411 (3.01)	496	13.8	0.42	3.1	4.2
	THF	420 (2.95)	511	16.2	0.38	2.3	3.8
	EtOAc	414 (2.99)	510	16.5	0.34	2.1	4.0
	CH_2Cl_2	415 (2.98)	533	13.2	0.27	2.0	5.5
	DMF	423 (2.93)	547	16.0	0.33	2.0	4.1
2b	toluene	423 (2.94)	508	13.0	0.45	3.5	4.2
	THF	424 (2.93)	521	15.0	0.51	3.4	3.3
	EtOAc	422 (2.94)	521	15.6	0.47	3.0	3.4
	CH_2Cl_2	425 (2.92)	548	14.6	0.34	2.3	4.5
	DMF	430 (2.89)	552	16.8	0.43	2.5	3.4
2c	toluene	424 (2.92)	508	13.5	0.55	4.1	3.4
	CH_2Cl_2	424 (2.92)	541	16.2	0.41	2.5	3.7

[a] Lifetime. [b] Radiative constant. [c] Non-radiative constant.

Table S3. Summary of Photophysical Data of **3a**,**b**, **4a**,**b**, and **5a**,**b**

	solv.	λ_{max}	λ_{em}	τ_f	Φ_f	k_r	k_{nr}
		[nm (eV)]	[nm]	[ns][a]		[10^7 s^{-1}][b]	[10^7 s^{-1}][c]
3a	toluene	410[d] (3.02)	456	1.02	0.07	7.3	91
	CH_2Cl_2	410[d] (3.02)	489	1.27	0.06	4.5	74
	DMF	410[d] (3.02)	493	1.30	0.05	3.8	73
3b	toluene	420[d] (2.95)	470	0.97	0.07	6.9	96
	CH_2Cl_2	420[d] (2.95)	497	1.00	0.04	4.3	95
	DMF	420[d] (2.95)	500	1.07	0.04	4.1	89
4a	toluene	406 (3.05)	472	1.50	0.11	7.2	60
	CH_2Cl_2	411 (3.01)	502	2.61	0.12	4.6	34
	DMF	412 (3.01)	507	2.29	0.09	3.9	40
4b	toluene	425[d] (2.91)	489	1.18	0.08	7.0	78
	CH_2Cl_2	430[d] (2.88)	515	1.81	0.07	3.9	51
	DMF	430[d] (2.91)	515	1.57	0.07	4.2	59
5a	toluene	425 (2.91)	501	9.48	0.50	5.3	5.3
	CH_2Cl_2	430 (2.88)	540	13.3	0.50	3.8	3.7
	DMF	436 (2.84)	544	16.1	0.47	2.9	3.3
5b	toluene	439 (2.83)	517	7.52	0.41	5.4	7.9
	CH_2Cl_2	440 (2.83)	553	12.6	0.44	3.4	4.5
	DMF	445 (2.78)	557	15.3	0.49	3.2	3.3

[a] Lifetime. [b] Radiative constant. [c] Non-radiative constant. [d] Peak as shoulder.

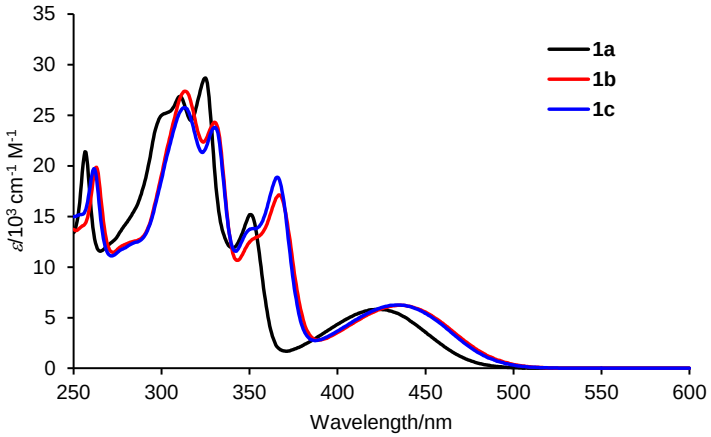

Figure S2. UV–vis absorption spectra of **1a**–**c** in CH_2Cl_2 at 298 K.

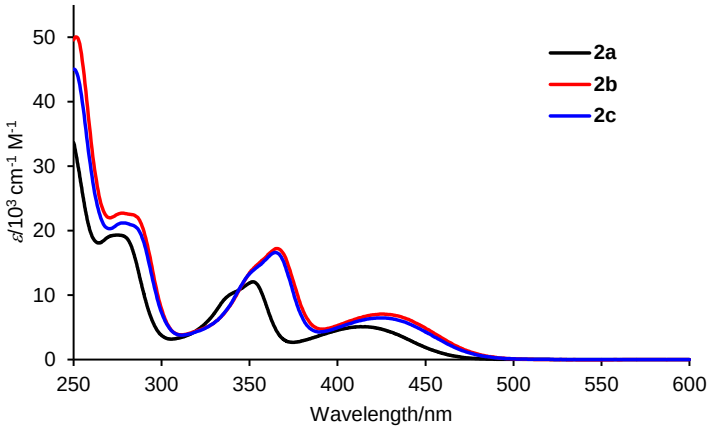

Figure S3. UV–vis absorption spectra of **2a**–**c** in CH_2Cl_2 at 298 K.

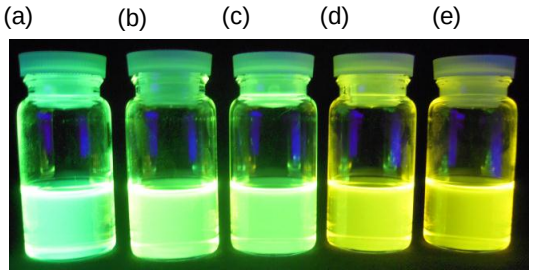

Figure S4. Fluorescent images under UV light (365 nm) for **1b** in (a) toluene, (b) THF, (c) EtOAc, (d) CH_2Cl_2, and (e) DMF.

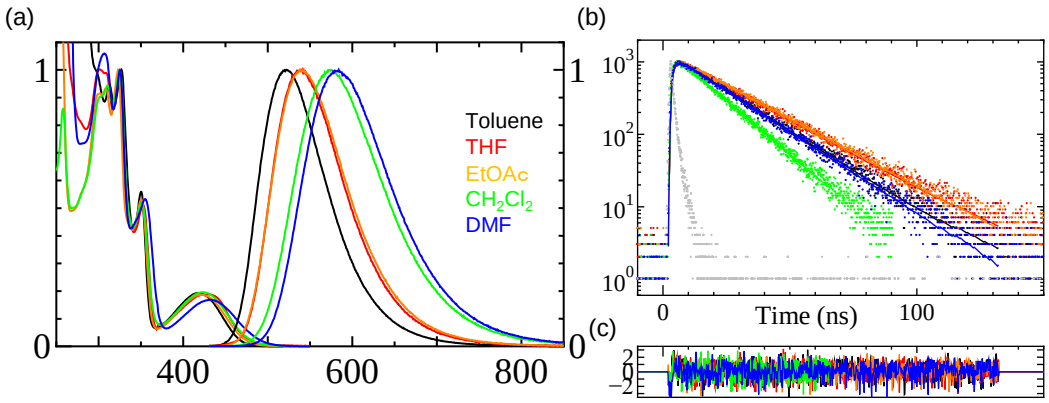

Figure S5. (a) UV–vis and fluorescence spectra of **1a**. (b) Fluorescence decay curves measured by time-correlated single-photon counting measurement. (c) Residual of fluorescence decay.

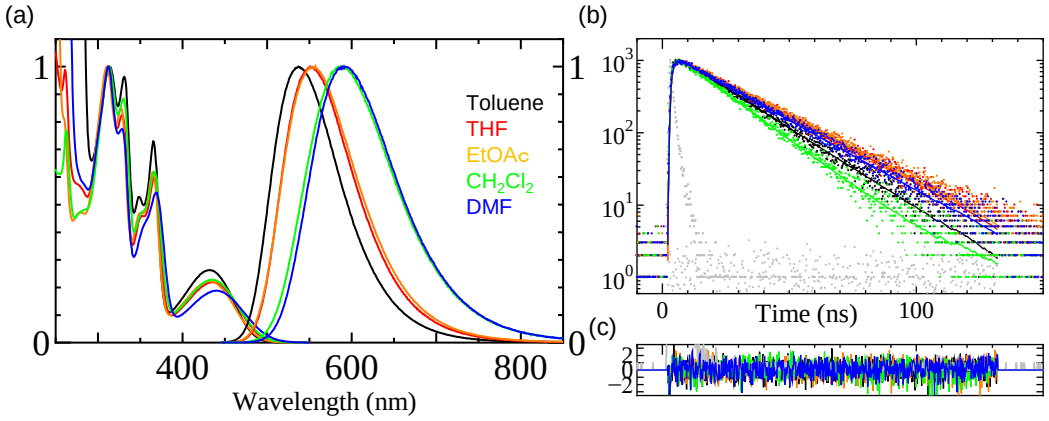

Figure S6. (a) UV–vis and fluorescence spectra of **1b**. (b) Fluorescence decay curves measured by time-correlated single-photon counting measurement. (c) Residual of fluorescence decay.

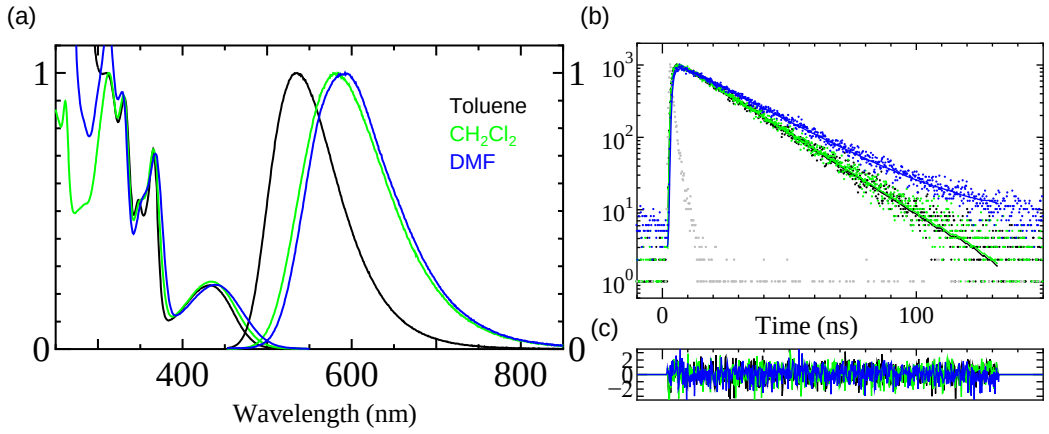

Figure S7. (a) UV–vis and fluorescence spectra of **1c**. (b) Fluorescence decay curves measured by time-correlated single-photon counting measurement. (c) Residual of fluorescence decay.

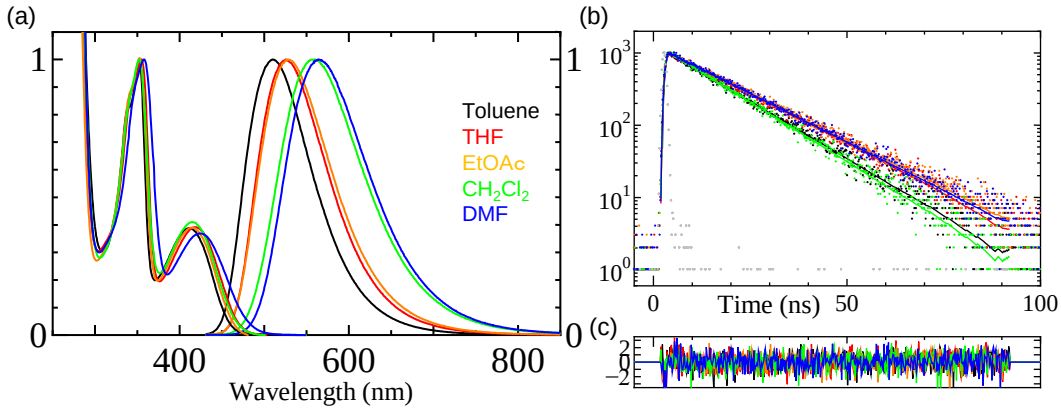

Figure S8. (a) UV–vis and fluorescence spectra of **2a**. (b) Fluorescence decay curves measured by time-correlated single-photon counting measurement. (c) Residual of fluorescence decay.

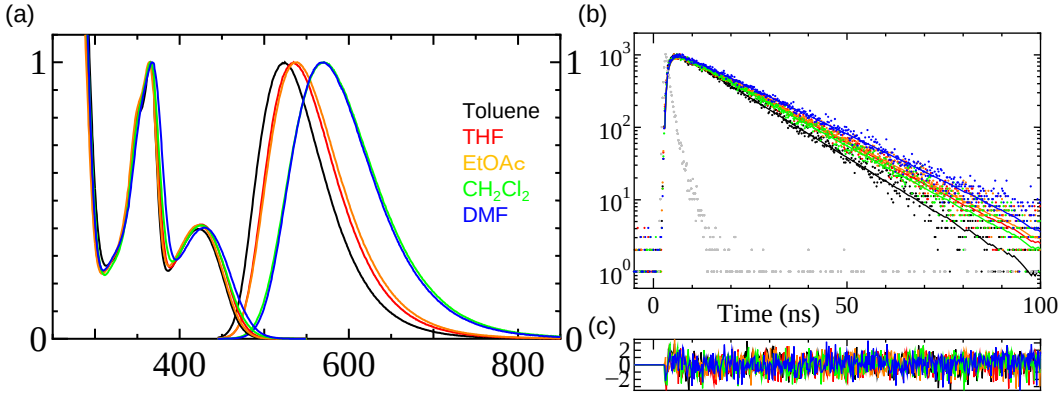

Figure S9. (a) UV–vis and fluorescence spectra of **2b**. (b) Fluorescence decay curves measured by time-correlated single-photon counting measurement. (c) Residual of fluorescence decay.

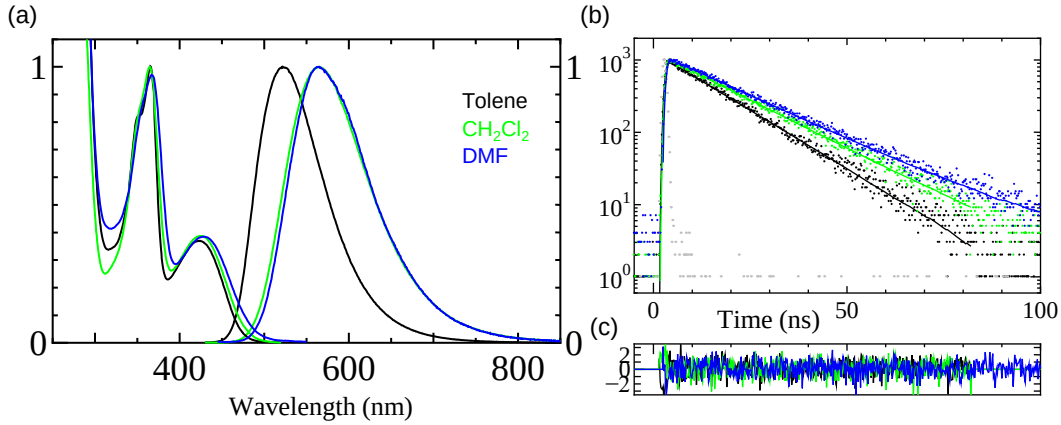

Figure S10. (a) UV–vis and fluorescence spectra of **2c**. (b) Fluorescence decay curves measured by time-correlated single-photon counting measurement. (c) Residual of fluorescence decay.

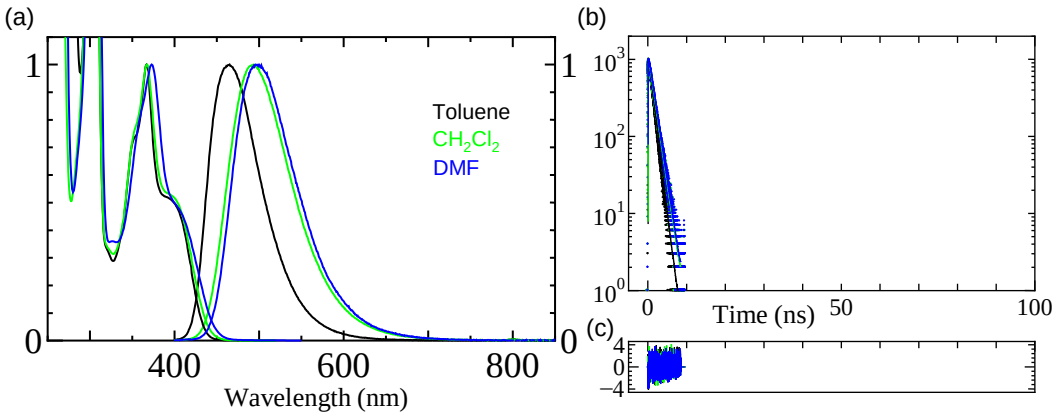

Figure S11. (a) UV–vis and fluorescence spectra of **3a**. (b) Fluorescence decay curves measured by time-correlated single-photon counting measurement. (c) Residual of fluorescence decay.

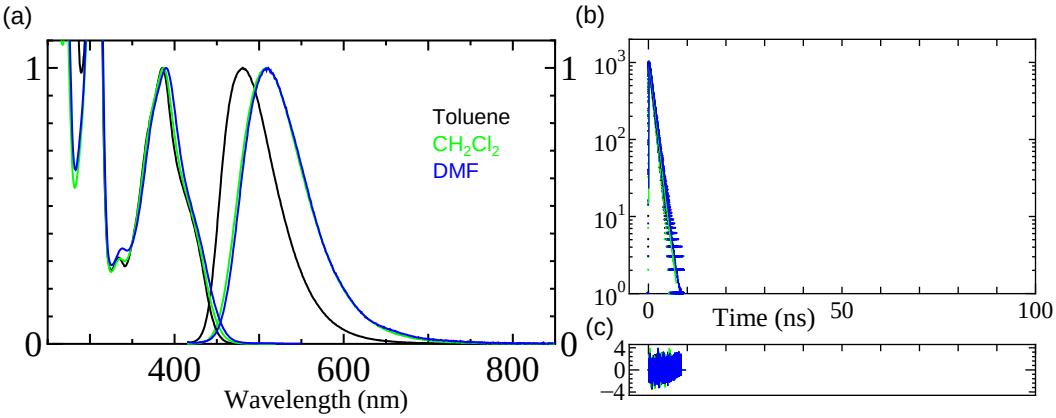

Figure S12. (a) UV–vis and fluorescence spectra of **3b**. (b) Fluorescence decay curves measured by time-correlated single-photon counting measurement. (c) Residual of fluorescence decay.

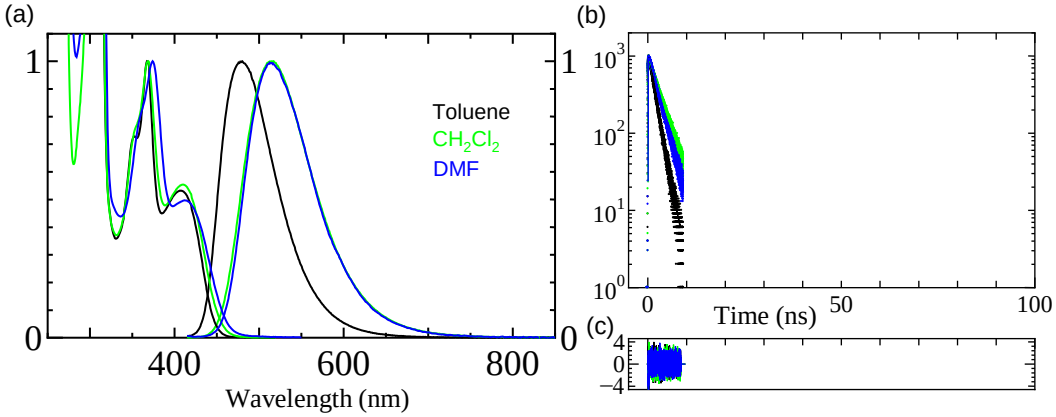

Figure S13. (a) UV–vis and fluorescence spectra of **4a**. (b) Fluorescence decay curves measured by time-correlated single-photon counting measurement. (c) Residual of fluorescence decay.

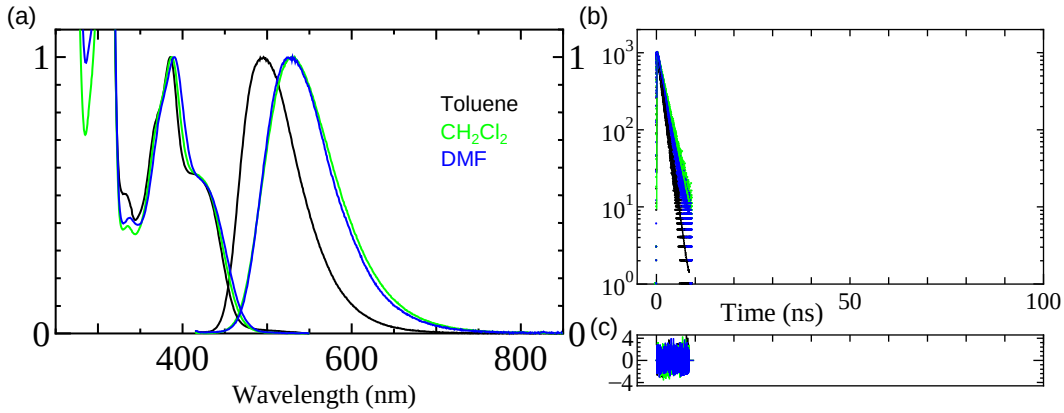

Figure S14. (a) UV–vis and fluorescence spectra of **4b**. (b) Fluorescence decay curves measured by time-correlated single-photon counting measurement. (c) Residual of fluorescence decay.

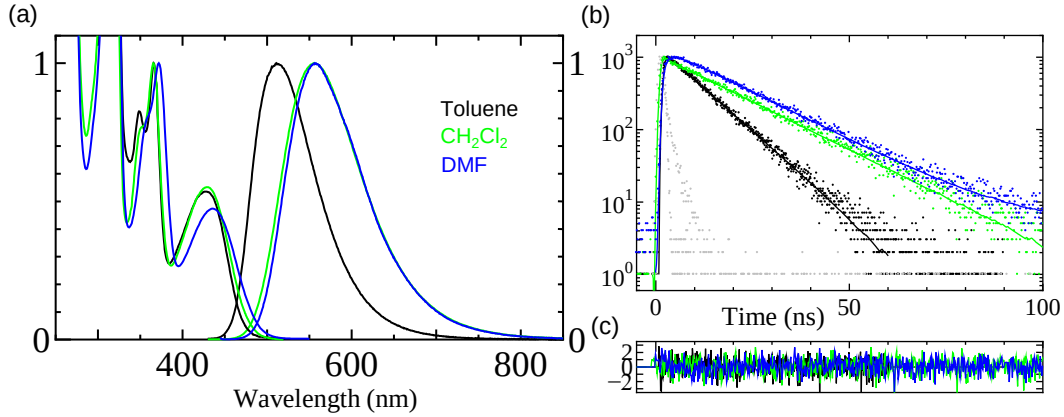

Figure S15. (a) UV–vis and fluorescence spectra of **5a**. (b) Fluorescence decay curves measured by time-correlated single-photon counting measurement. (c) Residual of fluorescence decay.

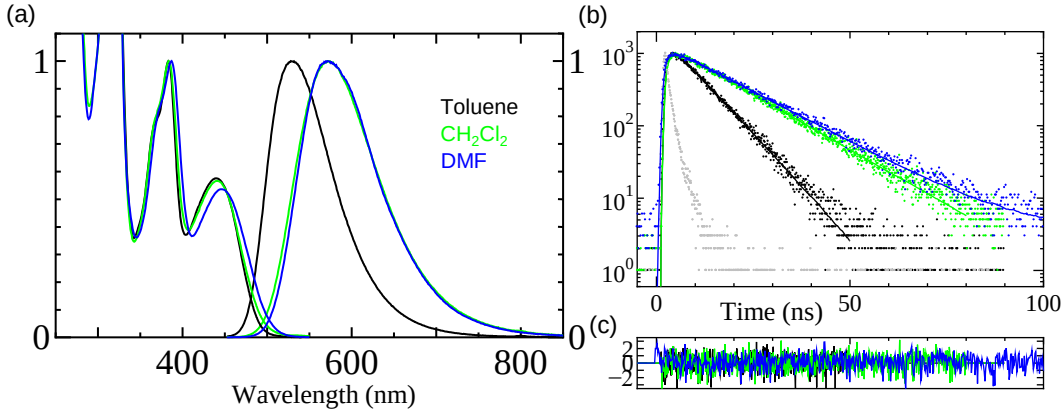

Figure S16. (a) UV–vis and fluorescence spectra of **5b**. (b) Fluorescence decay curves measured by time-correlated single-photon counting measurement. (c) Residual of fluorescence decay.

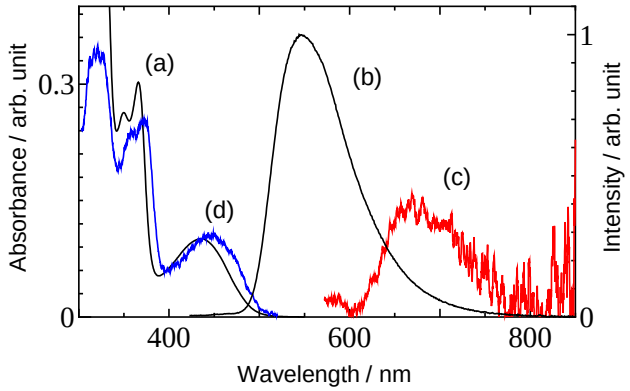

Figure S17. (a) UV–vis, (b) total emission, (c) phosphorescence, and (d) phosphorescence excitation (λ_{ex} = 650 nm) spectra of **1b** in 2-methyltetrahydrofuran matrix at 77 K.

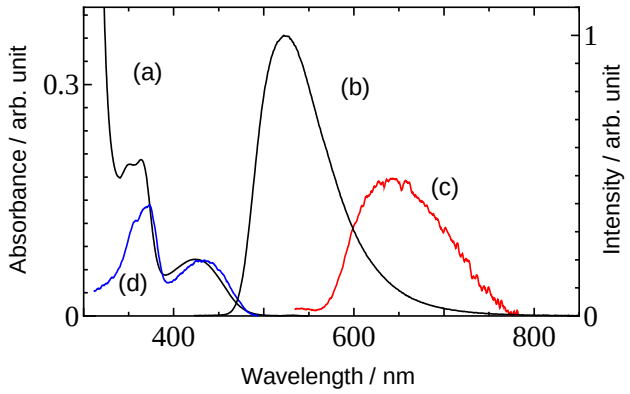

Figure S18. (a) UV–vis, (b) total emission, (c) phosphorescence, and (d) phosphorescence excitation (λ_{em} = 610 nm) spectra of **2b** in 2-methyltetrahydrofuran matrix at 77 K.

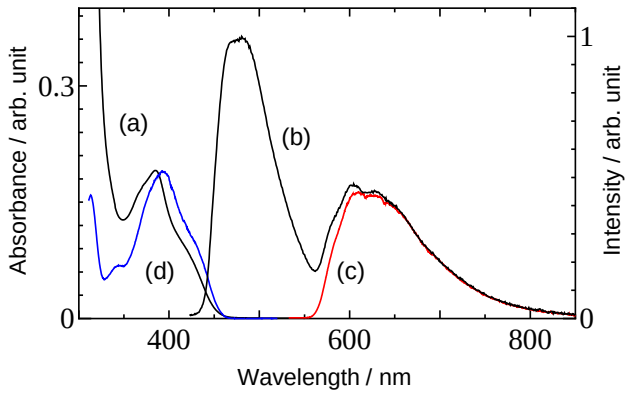

Figure S19. (a) UV–vis, (b) total emission, (c) phosphorescence, and (d) phosphorescence excitation (λ_{em} = 600 nm) spectra of **3b** in 2-methyltetrahydrofuran matrix at 77 K.

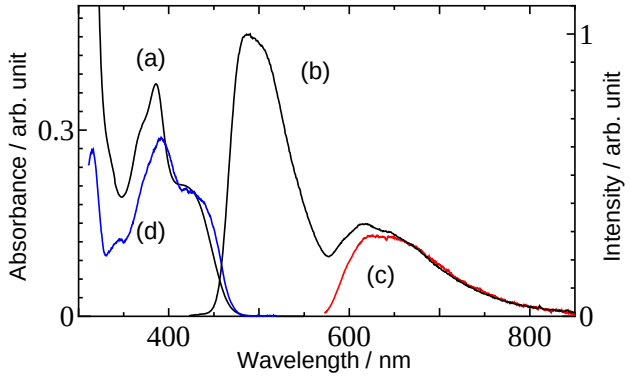

Figure S20. (a) UV–vis, (b) total emission, (c) phosphorescence, and (d) phosphorescence excitation (λ_{em} = 620 nm) spectra of **4b** in 2-methyltetrahydrofuran matirx at 77K.

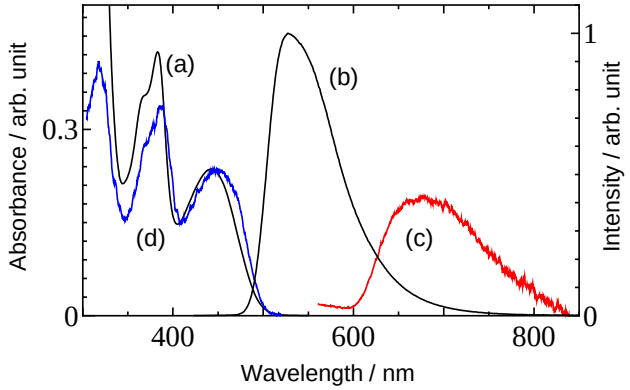

Figure S21. (a) UV-vis, (b) total emission, (c) phosphorescence, and (d) phosphorescence excitation (λ_{em} = 640 nm) spectra of **5b** in 2-methyltetrahydrofuran matrix at 77K.

Time-resolved photoacoustic (PA) measurements

Time-resolved photoacoustic (PA) measurements were performed using a Nd^{3+}: YAG laser (center wavelength: 266 nm; pulse width: 6 ns) as the excitation source. The sample solution was irradiated with the laser beam after passing through a 0.5-mm-wide slit. The effective acoustic transit time was estimated to be ca. 340 ns. The laser fluence was varied using a neutral density filter and the laser pulse energy was measured with a pyroelectric energy meter. The PA signal detected by a piezoelectric detector (1 MHz) was amplified using a wide-band high-input impedance amplifier (50 kHz, 40 dB) and fed to a digitizing oscilloscope. The sample solution temperature was controlled to within ±0.02 °C. Further detail is described in the literature.[10]

4. CV Data

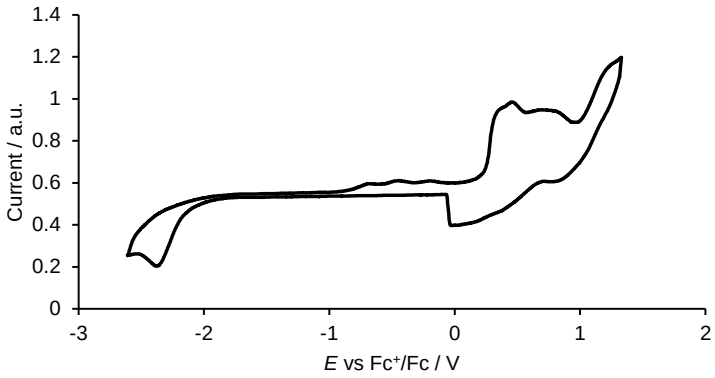

Figure S22. Cyclic voltammogram of **1a**.

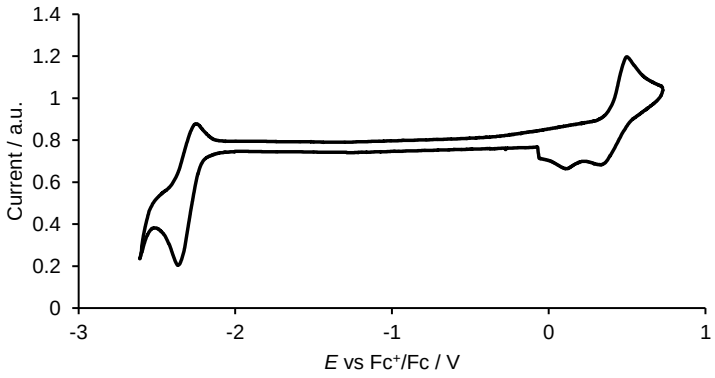

Figure S23. Cyclic voltammogram of **1c**.

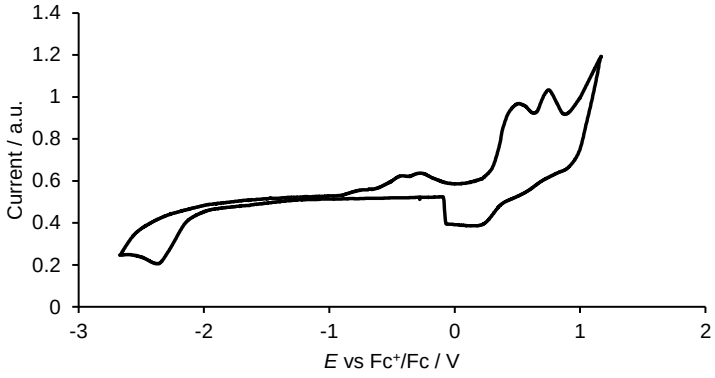

Figure S24. Cyclic voltammogram of **2a**.

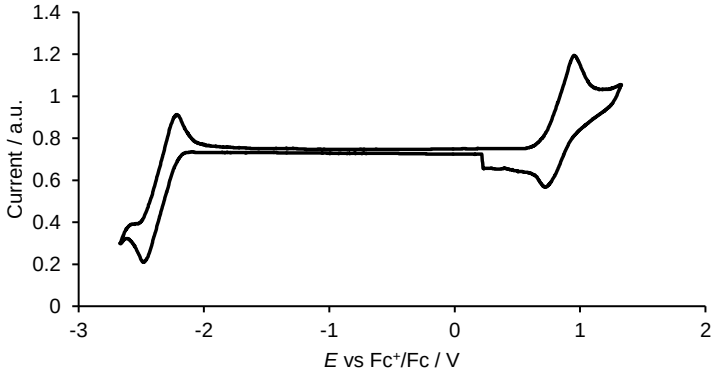

Figure S25. Cyclic voltammogram of **2b**.

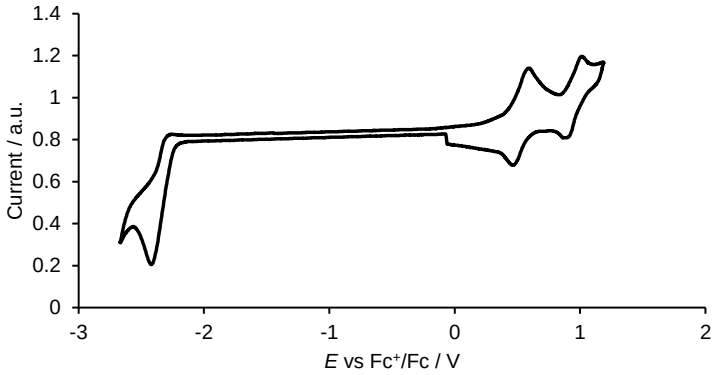

Figure S26. Cyclic voltammogram of **2c**.

5. Theoretical Calculations for 1b–5b

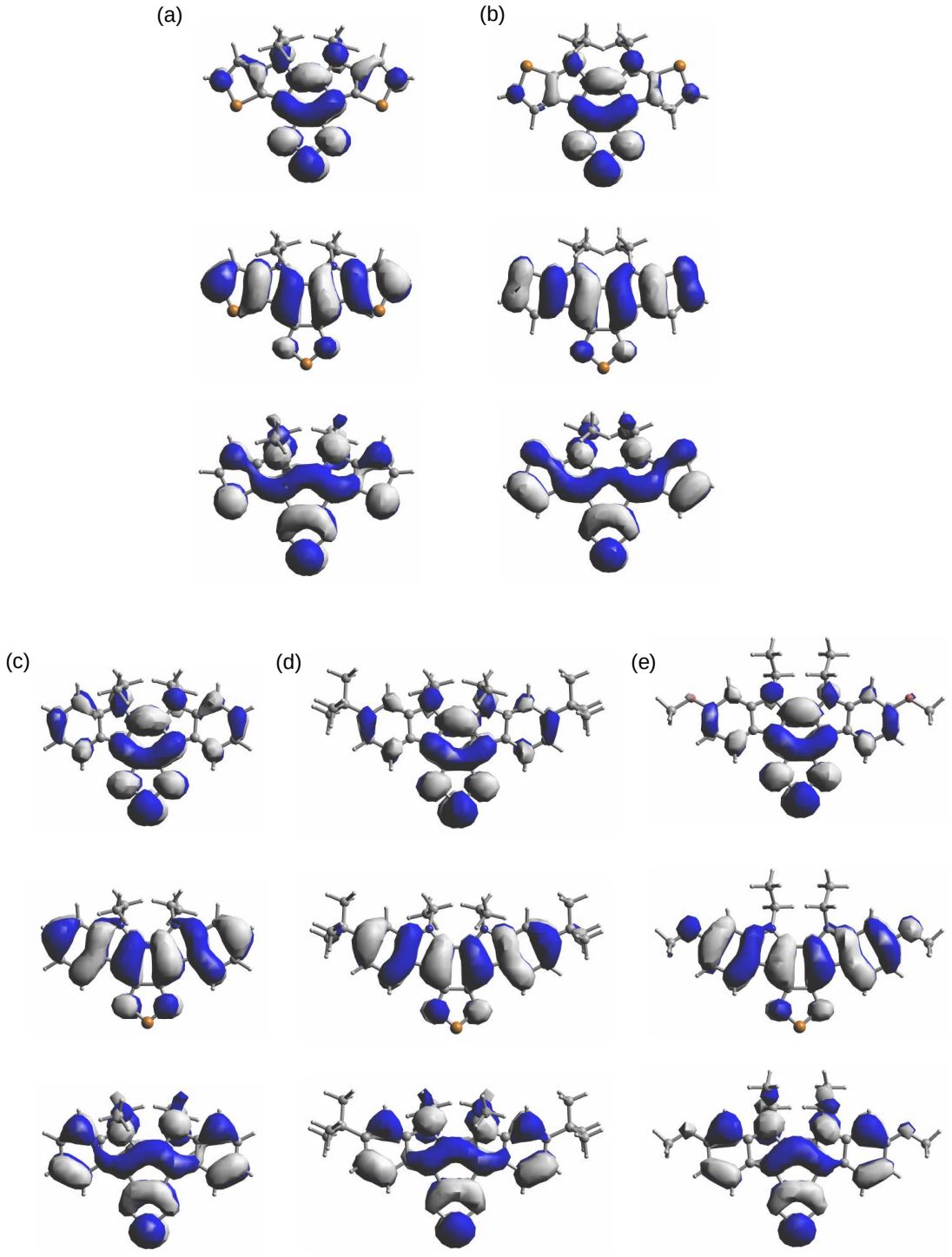

Figure S27. Molecular orbital plots of (a) **1b**, (b) **2b**, (c) **3b**, (d) **4b**, and (e) **5b** calculated by B3LYP/6-311G**//B3LYP/6-31G*. The upper, middle, and lower plots represent the LUMOs, HOMOs, and HOMO–1s, respectively.

Table S4. Selected Data of Electronic Transitions in **1b** by TDDFT Method at the B3LYP/6-31G*/B3LYP/6-31G* level[a][b]

State	λ [nm (eV)]	f	Composition of band and CI coefficiencies
1	458 (2.70)	0.1364	H→L, 0.65; H→L+1, –0.12
2	343 (3.60)	0.1902	H–1→L, 0.64; H→L+4, 0.12
3	327 (3.78)	0.0740	H–2→L, 0.58; H→L+1, –0.37
4	312 (3.96)	0.5095	H–2→L, 0.36; H→L+1, 0.53

[a] Calculations were carried out for the lowest 20 excited states, and only energies above 300 nm with f > 0.01 are shown. [b] f = oscillator strength; CI = configuration interaction; H = HOMO; L = LUMO.

Table S5. Selected Data of Electronic Transitions in **2b** by TDDFT Method at the B3LYP/6-31G*/B3LYP/6-31G* level[a][b]

State	λ [nm (eV)]	f	Composition of band and CI coefficiencies
1	441 (2.80)	0.1140	H→L, 0.67
2	351 (3.52)	0.1654	H–1→L, 0.65; H→L+1, –0.10
3	331 (3.73)	0.0264	H–2→L, 0.68

[a] Calculations were carried out for the lowest 20 excited states, and only energies above 300 nm with f > 0.01 are shown. [b] f = oscillator strength; CI = configuration interaction; H = HOMO; L = LUMO.

Table S6. Selected Data of Electronic Transitions in **3b** by TDDFT Method at the B3LYP/6-31G*/B3LYP/6-31G* level[a][b]

State	λ [nm (eV)]	f	Composition of band and CI coefficiencies
1	425 (2.91)	0.1496	H→L, 0.65; H→L+1, –0.10
2	366 (3.38)	0.1866	H–1→L, 0.64; H→L+4, –0.12
3	340 (3.64)	0.0465	H–2→L, 0.68

[a] Calculations were carried out for the lowest 20 excited states, and only energies above 300 nm with f > 0.01 are shown. [b] f = oscillator strength; CI = configuration interaction; H = HOMO; L = LUMO.

Table S7. Selected Data of Electronic Transitions in **4b** by TDDFT Method at the B3LYP/6-31G*/B3LYP/6-31G* level[a][b]

State	λ [nm (eV)]	f	Composition of band and CI coefficiencies
1	436 (2.83)	0.2063	H→L, 0.66
2	366 (3.34)	0.1829	H–1→L, 0.64; H→L+4, 0.11
3	341 (3.66)	0.0504	H–2→L, 0.68

[a] Calculations were carried out for the lowest 20 excited states, and only energies above 300 nm with f > 0.01 are shown. [b] f = oscillator strength; CI = configuration interaction; H = HOMO; L = LUMO.

Table S8. Selected Data of Electronic Transitions in **5b** by TDDFT Method at the B3LYP/6-31G*/B3LYP/6-31G* level[a][b]

State	λ [nm (eV)]	f	Composition of band and CI coefficiencies
1	476 (2.60)	0.1696	H→L, 0.66
2	372 (3.32)	0.1642	H–1→L, 0.65
3	331 (3.74)	0.0326	H–2→L, 0.67; H→L+1, –0.13

[a] Calculations were carried out for the lowest 20 excited states, and only energies above 300 nm with f > 0.01 are shown. [b] f = oscillator strength; CI = configuration interaction; H = HOMO; L = LUMO.

Table S9. Cartesian Coordinates from the Optimized Structure of **1b** at B3LYP/6-31G*

Center Number	Atomic Number	Atomic Type	Coordinates (Angstroms) X	Y	Z
1	6	0	0.715629	-0.618148	-0.014987
2	6	0	-0.715617	-0.618006	0.014686
3	6	0	-1.420729	0.597152	0.171380
4	6	0	-0.717269	1.841364	0.123409
5	6	0	0.717752	1.841223	-0.123696
6	6	0	1.420972	0.596870	-0.171627
7	7	0	-1.246801	3.057156	0.215334
8	16	0	0.000469	4.128993	-0.000164
9	7	0	1.247531	3.056906	-0.215625
10	7	0	-1.623768	-1.683917	-0.057120
11	6	0	-2.897845	-1.130454	0.095537
12	6	0	-2.796229	0.246943	0.250940
13	6	0	2.796426	0.246417	-0.251072
14	6	0	2.897780	-1.130986	-0.095641
15	7	0	1.623579	-1.684274	0.056832
16	6	0	-4.234311	-1.622081	0.095512
17	6	0	-5.123829	-0.594444	0.269102
18	16	0	-4.359954	0.977414	0.427502
19	16	0	4.360300	0.976625	-0.427381
20	6	0	5.123888	-0.595349	-0.268733
21	6	0	4.234161	-1.622835	-0.095309
22	6	0	-1.441577	-2.858644	-0.928730
23	6	0	1.441367	-2.858650	0.928936
24	6	0	1.855916	-2.605641	2.382209
25	6	0	-1.858124	-2.606880	-2.381652
26	1	0	-4.529643	-2.659549	-0.011838
27	1	0	-6.201532	-0.664063	0.332156
28	1	0	6.201592	-0.665145	-0.331569
29	1	0	4.529307	-2.660343	0.012161
30	1	0	-2.017099	-3.685497	-0.497214
31	1	0	-0.390928	-3.144682	-0.903395
32	1	0	2.018294	-3.685102	0.498553
33	1	0	0.391079	-3.145907	0.902416
34	1	0	1.686850	-3.509842	2.977969
35	1	0	1.263414	-1.793646	2.815844
36	1	0	2.913729	-2.337397	2.456939
37	1	0	-1.688792	-3.511247	-2.977084
38	1	0	-1.266977	-1.794510	-2.816432
39	1	0	-2.916296	-2.339788	-2.455340

Item	Value	Threshold	Converged?
Maximum Force	0.000070	0.000450	YES
RMS Force	0.000012	0.000300	YES
Maximum Displacement	0.001482	0.001800	YES
RMS Displacement	0.000282	0.001200	YES

Predicted change in Energy=-9.000159D-08
Optimization completed.
-- Stationary point found.
Sum of electronic and zero-point Energies= -2107.606925
Sum of electronic and thermal Energies= -2107.585845
Sum of electronic and thermal Enthalpies= -2107.584901
Sum of electronic and thermal Free Energies= -2107.657517

Table S10. Cartesian Coordinates from the Optimized Structure of **2b** at B3LYP/6-31G*

Center Number	Atomic Number	Atomic Type	Coordinates (Angstroms) X	Y	Z
1	6	0	0.722361	-0.409151	-0.012500
2	6	0	-0.722369	-0.409150	0.012500
3	6	0	-1.419368	0.820321	0.108550
4	6	0	-0.720256	2.064970	0.078310
5	6	0	0.720254	2.064969	-0.078300
6	6	0	1.419362	0.820318	-0.108550
7	7	0	-1.258335	3.280961	0.137000
8	16	0	-0.000014	4.352579	0.000010
9	7	0	1.258335	3.280958	-0.136980
10	7	0	-1.678181	-1.447639	-0.024510
11	6	0	-2.917450	-0.843977	0.057750
12	6	0	-2.816348	0.532003	0.154840
13	6	0	2.816342	0.531996	-0.154850
14	6	0	2.917450	-0.843984	-0.057780
15	7	0	1.678179	-1.447643	0.024490
16	16	0	-4.561501	-1.412515	0.064120
17	6	0	-5.115399	0.262116	0.202730
18	6	0	-4.097257	1.167094	0.241170
19	6	0	4.097243	1.167105	-0.241220
20	6	0	5.115391	0.262123	-0.202810
21	16	0	4.561489	-1.412506	-0.064200
22	6	0	-1.553542	-2.810339	-0.554200
23	6	0	1.553548	-2.810302	0.554310
24	6	0	1.032418	-2.858412	1.992240
25	6	0	-1.032352	-2.858569	-1.992110
26	1	0	-6.180548	0.444127	0.247170
27	1	0	-4.244246	2.237295	0.323440
28	1	0	4.244234	2.237314	-0.323470
29	1	0	6.180542	0.444142	-0.247270
30	1	0	-2.557803	-3.240638	-0.513930
31	1	0	-0.944983	-3.416599	0.117980
32	1	0	2.557827	-3.240604	0.514040
33	1	0	0.944977	-3.416632	-0.117800
34	1	0	0.026268	-2.436111	2.073300
35	1	0	1.692798	-2.292383	2.656590
36	1	0	0.998836	-3.896512	2.341700
37	1	0	-0.998744	-3.896709	-2.341480
38	1	0	-0.026202	-2.436271	-2.073170
39	1	0	-1.692702	-2.292599	-2.656530

Item	Value	Threshold	Converged?
Maximum Force	0.000009	0.000450	YES
RMS Force	0.000002	0.000300	YES
Maximum Displacement	0.001665	0.001800	YES
RMS Displacement	0.000318	0.001200	YES

Predicted change in Energy=-1.453689D-08
Optimization completed.
-- Stationary point found.
Sum of electronic and zero-point Energies= -2107.598410
Sum of electronic and thermal Energies= -2107.577544
Sum of electronic and thermal Enthalpies= -2107.576600
Sum of electronic and thermal Free Energies= -2107.648113

Table S11. Cartesian Coordinates from the Optimized Structure of **3b** at B3LYP/6-31G*

Center Number	Atomic Number	Atomic Type	Coordinates (Angstroms) X	Y	Z
1	6	0	-0.716481	-0.520608	0.012007
2	6	0	0.716386	-0.520705	-0.011878
3	6	0	1.420832	0.681238	-0.169229
4	6	0	0.718777	1.926192	-0.123373
5	6	0	-0.718424	1.926339	0.123228
6	6	0	-1.420736	0.681544	0.169137
7	7	0	1.247175	3.143924	-0.215553
8	16	0	0.000422	4.215122	-0.000124
9	7	0	-1.246576	3.144194	0.215261
10	7	0	1.617958	-1.589995	0.066685
11	6	0	2.905812	-1.053002	-0.089832
12	6	0	2.817805	0.351989	-0.252047
13	6	0	-2.817770	0.352603	0.251580
14	6	0	-2.906029	-1.052407	0.089488
15	7	0	-1.618295	-1.589519	-0.066680
16	6	0	4.138433	-1.710841	-0.084419
17	6	0	5.284734	-0.940646	-0.269261
18	6	0	5.208769	0.453465	-0.445687
19	6	0	3.983048	1.110144	-0.437273
20	6	0	-3.982947	1.111027	0.436179
21	6	0	-5.208802	0.454605	0.444219
22	6	0	-5.284989	-0.939522	0.267962
23	6	0	-4.138800	-1.709999	0.083665
24	6	0	1.820885	-2.491144	2.404830
25	6	0	1.415410	-2.752766	0.950162
26	6	0	-1.821392	-2.495799	-2.402658
27	6	0	-1.415562	-2.754114	-0.947512
28	1	0	4.208753	-2.786522	0.047742
29	1	0	6.255280	-1.429006	-0.279968
30	1	0	6.122895	1.022726	-0.589076
31	1	0	3.914956	2.185511	-0.565522
32	1	0	-3.914661	2.186397	0.564300
33	1	0	-6.122876	1.024069	0.587131
34	1	0	-6.255644	-1.427674	0.278305
35	1	0	-4.209319	-2.785673	-0.048453
36	1	0	1.634073	-3.387271	3.007412
37	1	0	2.881053	-2.235998	2.487430
38	1	0	1.234546	-1.667929	2.825848

39	1	0	0.361183	-3.024546	0.919369
40	1	0	1.980463	-3.593988	0.533952
41	1	0	-1.634953	-3.393403	-3.003172
42	1	0	-1.235013	-1.673719	-2.825827
43	1	0	-2.881531	-2.240617	-2.485548
44	1	0	-1.980299	-3.594601	-0.529355
45	1	0	-0.361253	-3.025485	-0.916309

Item	Value	Threshold	Converged?
Maximum Force	0.000030	0.000450	YES
RMS Force	0.000005	0.000300	YES
Maximum Displacement	0.001080	0.001800	YES
RMS Displacement	0.000259	0.001200	YES

Predicted change in Energy=-2.711972D-08
Optimization completed.
-- Stationary point found.
Sum of electronic and zero-point Energies= -1466.051952
Sum of electronic and thermal Energies= -1466.030525
Sum of electronic and thermal Enthalpies= -1466.029581
Sum of electronic and thermal Free Energies= -1466.102198

Table S12. Cartesian Coordinates from the Optimized Structure of **4b** at B3LYP/6-31G*

Center Number	Atomic Number	Atomic Type	Coordinates (Angstroms) X	Y	Z
1	6	0	0.728444	-0.016031	-0.020962
2	6	0	-0.715059	-0.024877	0.011250
3	6	0	-1.414283	1.190264	0.142034
4	6	0	-0.726197	2.440379	0.104225
5	6	0	0.709551	2.449020	-0.104956
6	6	0	1.412291	1.207429	-0.146902
7	7	0	-1.267593	3.653981	0.184146
8	16	0	-0.021651	4.733252	0.003465
9	7	0	1.236739	3.669227	-0.180850
10	7	0	-1.652137	-1.069990	-0.055895
11	6	0	-2.931221	-0.506193	0.032220
12	6	0	-2.813928	0.891619	0.180693
13	6	0	2.816687	0.926522	-0.186671
14	6	0	2.950287	-0.472997	-0.045239
15	7	0	1.676777	-1.052543	0.040369
16	6	0	-4.181477	-1.130907	-0.062642
17	6	0	-5.340468	-0.355880	0.034178
18	6	0	-5.208378	1.043813	0.217172
19	6	0	-3.974558	1.672193	0.283789
20	6	0	3.965494	1.719363	-0.283138
21	6	0	5.212705	1.107636	-0.216954
22	6	0	5.360228	-0.286840	-0.043253
23	6	0	4.205666	-1.077375	0.046619
24	6	0	-6.749240	-0.973963	-0.046344
25	6	0	-6.714880	-2.498802	-0.263293
26	6	0	-7.508699	-0.695180	1.273149
27	6	0	-7.525822	-0.342276	-1.226681
28	6	0	6.742742	-0.964615	0.047481
29	6	0	6.873349	-1.698312	1.403734
30	6	0	7.901487	0.045610	-0.058295
31	6	0	6.894771	-1.987828	-1.103528

32	6	0	-1.769821	-3.583367	0.166163
33	6	0	-1.460174	-2.366766	-0.712757
34	6	0	1.824340	-3.567098	-0.151873
35	6	0	1.502150	-2.343951	0.713240
36	1	0	-4.250948	-2.200364	-0.209177
37	1	0	-6.102901	1.653554	0.301004
38	1	0	-3.896236	2.747928	0.401776
39	1	0	3.874881	2.794845	-0.394549
40	1	0	6.093283	1.734377	-0.293795
41	1	0	4.294881	-2.148620	0.185042
42	1	0	-7.738105	-2.886875	-0.318703
43	1	0	-6.210916	-3.018118	0.560137
44	1	0	-6.211023	-2.766725	-1.199321
45	1	0	-8.518440	-1.121978	1.230554
46	1	0	-7.608107	0.377605	1.467233
47	1	0	-6.986089	-1.141128	2.127065
48	1	0	-8.536141	-0.765366	-1.288301
49	1	0	-7.017120	-0.535810	-2.178000
50	1	0	-7.625495	0.742293	-1.117039
51	1	0	7.854721	-2.182089	1.483675
52	1	0	6.110496	-2.474911	1.524913
53	1	0	6.770850	-0.996771	2.239370
54	1	0	8.858591	-0.483858	0.009889
55	1	0	7.873951	0.784294	0.750493
56	1	0	7.888927	0.582784	-1.013241
57	1	0	7.871541	-2.484310	-1.048488
58	1	0	6.818361	-1.493910	-2.078825
59	1	0	6.123833	-2.764575	-1.062234
60	1	0	-1.597244	-4.501710	-0.406389
61	1	0	-2.810704	-3.586810	0.498871
62	1	0	-1.142903	-3.616375	1.061825
63	1	0	-0.434919	-2.402142	-1.078610
64	1	0	-2.105096	-2.388786	-1.601090
65	1	0	1.666792	-4.480489	0.432843
66	1	0	2.863612	-3.560704	-0.489558
67	1	0	1.194077	-3.619734	-1.044178
68	1	0	0.478193	-2.388026	1.081922
69	1	0	2.149382	-2.347797	1.600304

Item	Value	Threshold	Converged?
Maximum Force	0.000019	0.000450	YES
RMS Force	0.000003	0.000300	YES
Maximum Displacement	0.001625	0.001800	YES
RMS Displacement	0.000372	0.001200	YES

Predicted change in Energy=-2.251212D-08
Optimization completed.
-- Stationary point found.
Sum of electronic and zero-point Energies= -1780.335233
Sum of electronic and thermal Energies= -1780.302540
Sum of electronic and thermal Enthalpies= -1780.301596
Sum of electronic and thermal Free Energies= -1780.398257

Table S13. Cartesian Coordinates from the Optimized Structure of **5b** at B3LYP/6-31G*

Center Number	Atomic Number	Atomic Type	Coordinates (Angstroms) X	Y	Z

1	6	0	0.720890	-0.277358	0.008104
2	6	0	-0.720879	-0.277336	-0.008080
3	6	0	-1.415643	0.939787	-0.128689
4	6	0	-0.719523	2.184517	-0.095617
5	6	0	0.719526	2.184491	0.096294
6	6	0	1.415662	0.939762	0.129021
7	7	0	-1.254382	3.402186	-0.166892
8	16	0	0.000002	4.473309	0.000545
9	7	0	1.254380	3.402148	0.167835
10	7	0	-1.662257	-1.322383	0.062946
11	6	0	-2.938951	-0.755063	-0.012132
12	6	0	-2.818768	0.648327	-0.156771
13	6	0	2.818792	0.648342	0.156475
14	6	0	2.938953	-0.755023	0.011514
15	7	0	1.662274	-1.322333	-0.063158
16	6	0	-4.184603	-1.372613	0.093101
17	6	0	-5.325018	-0.566525	0.008571
18	6	0	-5.221173	0.829150	-0.167117
19	6	0	-3.971360	1.436196	-0.242880
20	6	0	3.971414	1.436201	0.242317
21	6	0	5.221202	0.829182	0.165974
22	6	0	5.325009	-0.566472	-0.009931
23	6	0	4.184579	-1.372561	-0.094215
24	8	0	-6.513514	-1.237909	0.108209
25	6	0	-7.718633	-0.494130	0.037534
26	8	0	6.513481	-1.237793	-0.110270
27	6	0	7.718641	-0.494278	-0.037633
28	6	0	-1.802403	-3.836545	-0.124816
29	6	0	-1.471873	-2.612175	0.735114
30	6	0	1.802426	-3.836295	0.127028
31	6	0	1.471749	-2.612734	-0.734017
32	1	0	-4.316232	-2.438613	0.231654
33	1	0	-6.112391	1.441388	-0.236219
34	1	0	-3.884299	2.511771	-0.355223
35	1	0	3.884394	2.511762	0.354832
36	1	0	6.112434	1.441437	0.234745
37	1	0	4.316156	-2.438536	-0.233015
38	1	0	-8.525091	-1.222486	0.143199
39	1	0	-7.821578	0.021209	-0.926652
40	1	0	-7.788830	0.243101	0.848344
41	1	0	8.525103	-1.222750	-0.142461
42	1	0	7.820338	0.020697	0.926868
43	1	0	7.790123	0.243236	-0.848089
44	1	0	-1.629877	-4.749159	0.456805
45	1	0	-1.186622	-3.884965	-1.027488
46	1	0	-2.847438	-3.835585	-0.444058
47	1	0	-2.106135	-2.617718	1.631524
48	1	0	-0.441925	-2.651097	1.087584
49	1	0	1.630551	-4.749457	-0.453931
50	1	0	1.186293	-3.884295	1.029480
51	1	0	2.847327	-3.834573	0.446703
52	1	0	2.105942	-2.619120	-1.630468
53	1	0	0.441779	-2.651976	-1.086381

Item	Value	Threshold	Converged?
Maximum Force	0.000031	0.000450	YES
RMS Force	0.000007	0.000300	YES
Maximum Displacement	0.001256	0.001800	YES
RMS Displacement	0.000276	0.001200	YES

Predicted change in Energy=-4.647487D-08
Optimization completed.
-- Stationary point found.
Sum of electronic and zero-point Energies= -1695.027382
Sum of electronic and thermal Energies= -1695.000747
Sum of electronic and thermal Enthalpies= -1694.999803
Sum of electronic and thermal Free Energies= -1695.083632

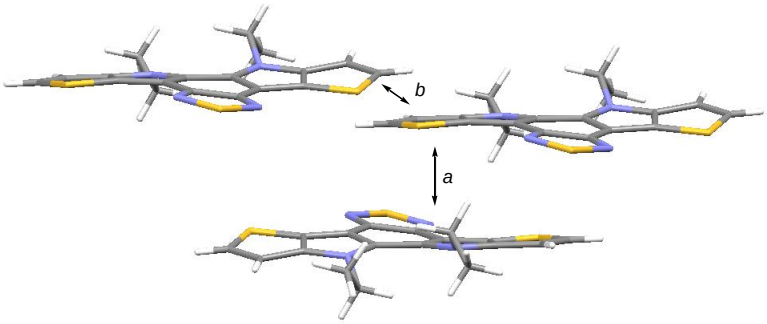

Table S14. Estimated Transfer Integrals of HOMO and LUMO Energy Levels between Neighboring Molecules of **1b**

	t_{HOMO}	t_{LUMO}
	[meV]	
a	151.4	43.2
b	6.4	1.2

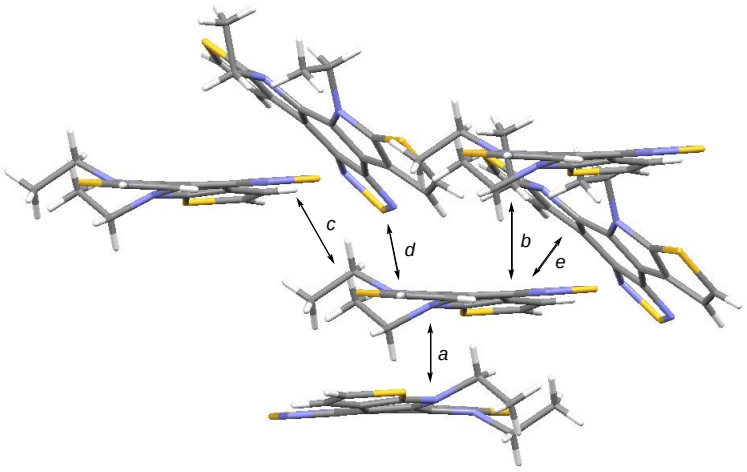

Table S15. Estimated Transfer Integrals of HOMO and LUMO Energy Levels between Neighboring Molecules of **2b**

	t_{HOMO}	t_{LUMO}
	[meV]	
a	102.7	16.9
b	27.0	26.7
c	7.9	7.2
d	14.5	19.3
e	14.5	19.3

6. Thermal Gravimetric Analysis

Table S16. Thermal Gravimetric Analysis of **1b**–**5b**

	M.p. [°C]	T_d [°C]	$T_{95\%}$ [°C]
1b	210–213	385	332
2b	187–190	325	304
3b	179–181	371	295
4b	200–204	395	301
5b	214–216	401	321

[a] Temperature at which melting occurred as observed by naked eye on a melting point apparatus. [b] Decomposition temperature determined by thermo-gravimetry. [c] Temperature at which 5% weight loss occurred upon heating.

7. Reported Synthesis of 1a, 3a, and 4a, and Attempted Synthesis of Furopyrrole-Fused Derivative

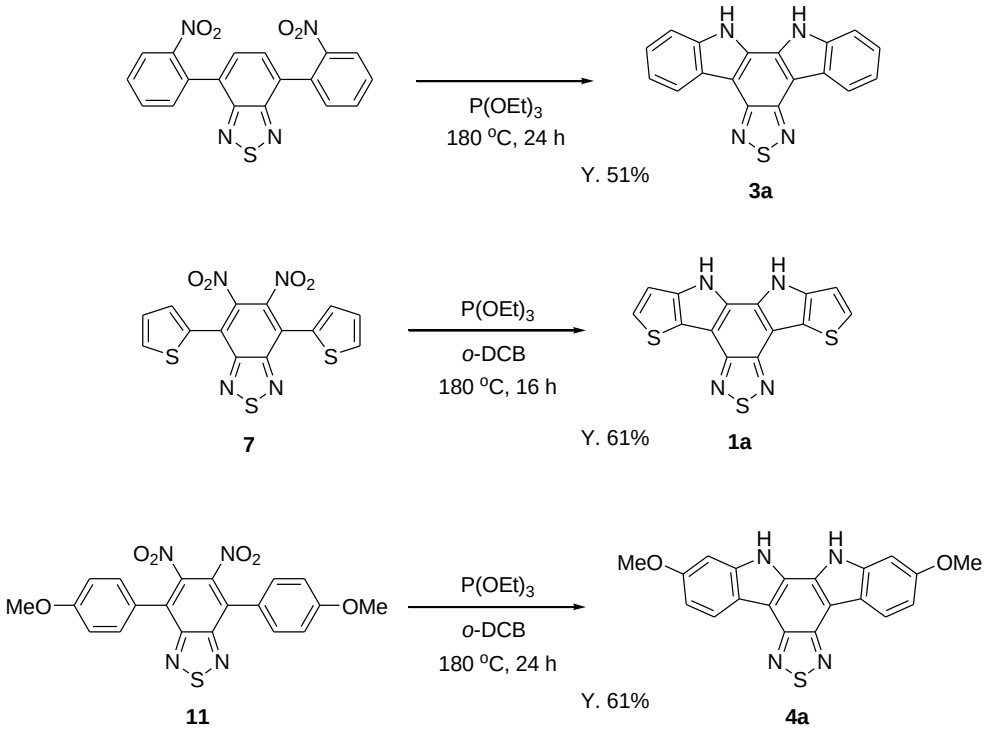

Scheme S1. Reported synthesis of **1a**,[3] **3a**,[11] and **4a**.[12]

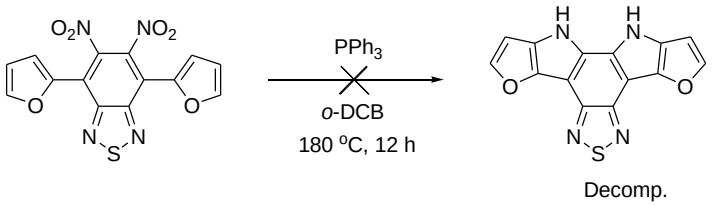

Scheme S2. Attempted synthesis of furopyrrole-fused derivative.

8. NMR Data

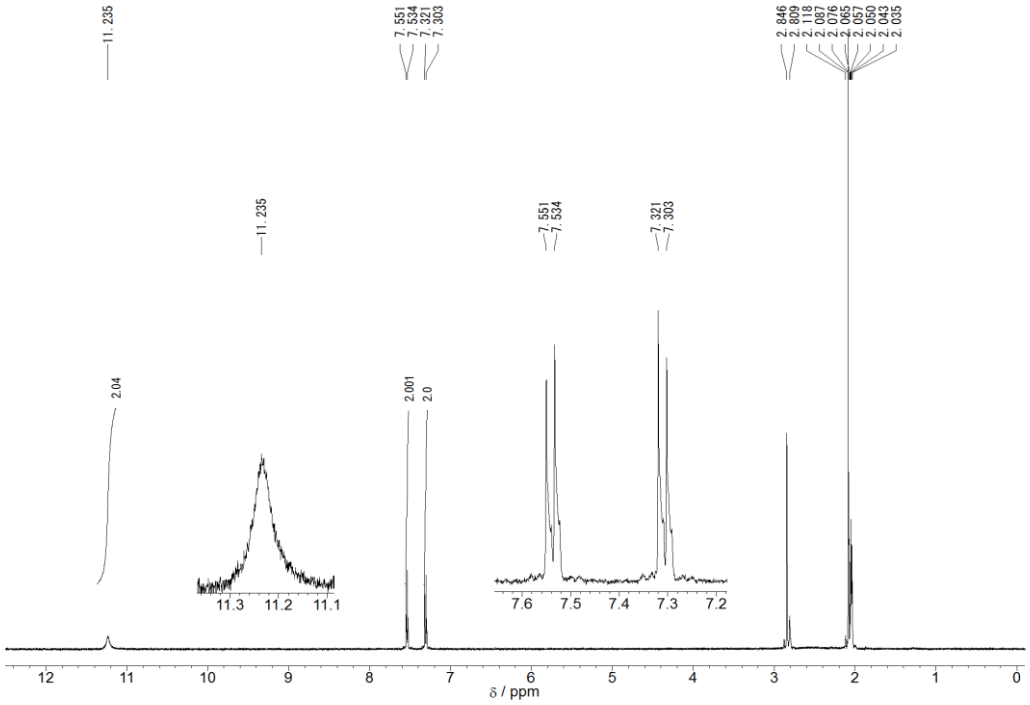

^{1}H NMR spectrum of **1a** in acetone-d_6 solution (300 MHz).

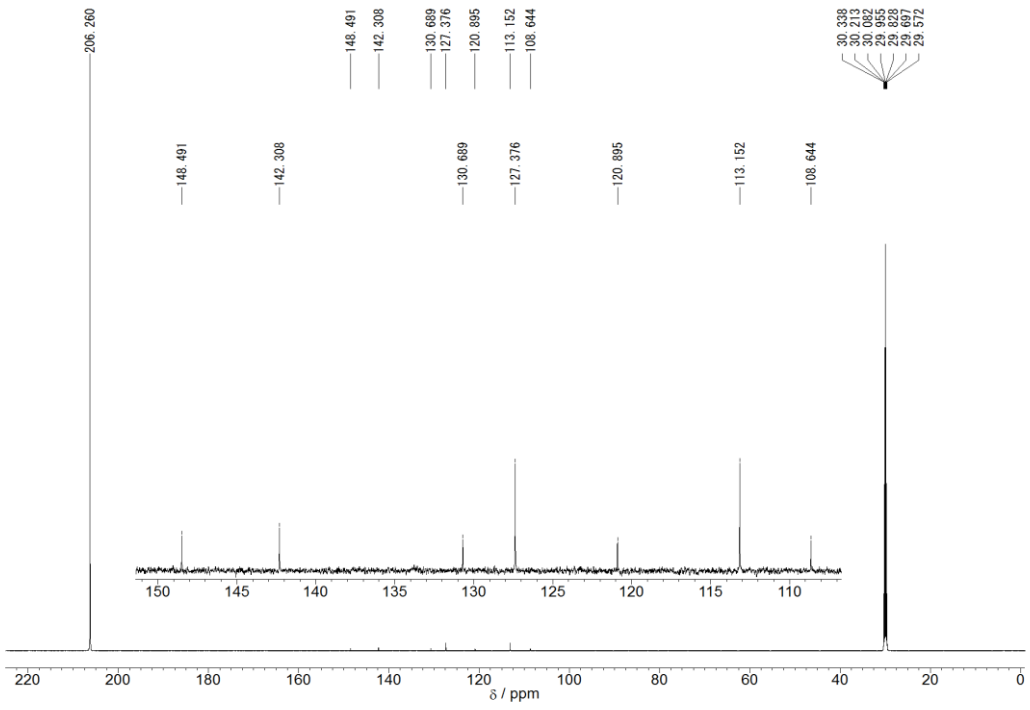

^{13}C NMR spectrum of **1a** in acetone-d_6 solution (150 MHz).

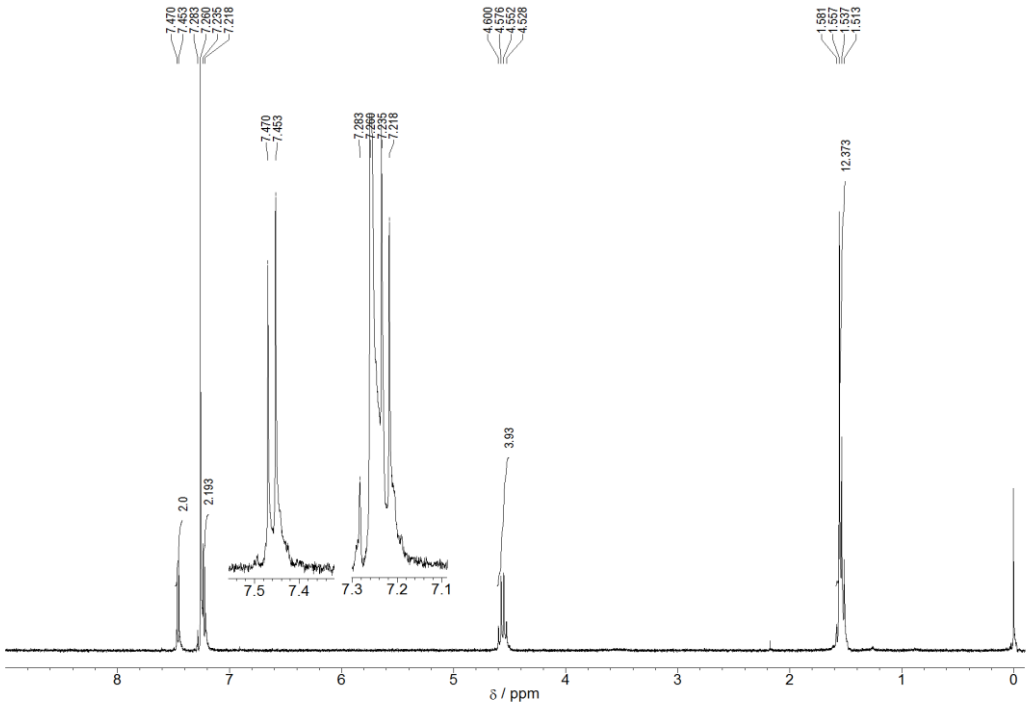

^{1}H NMR spectrum of **1b** in $CDCl_3$ solution (300 MHz).

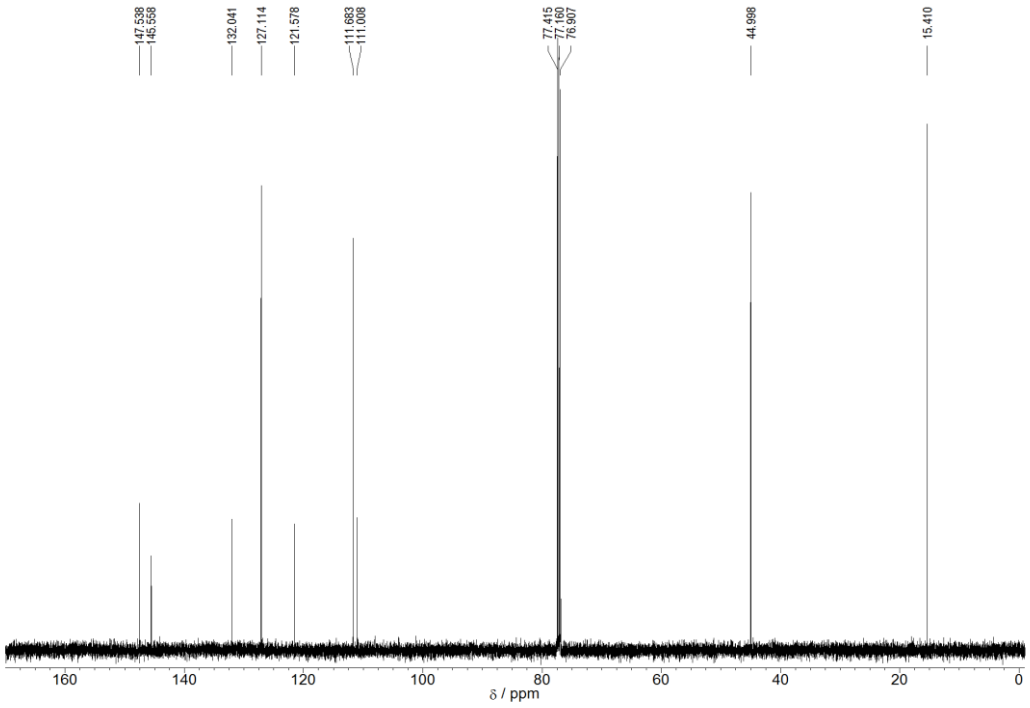

^{13}C NMR spectrum of **1b** in $CDCl_3$ solution (125 MHz).

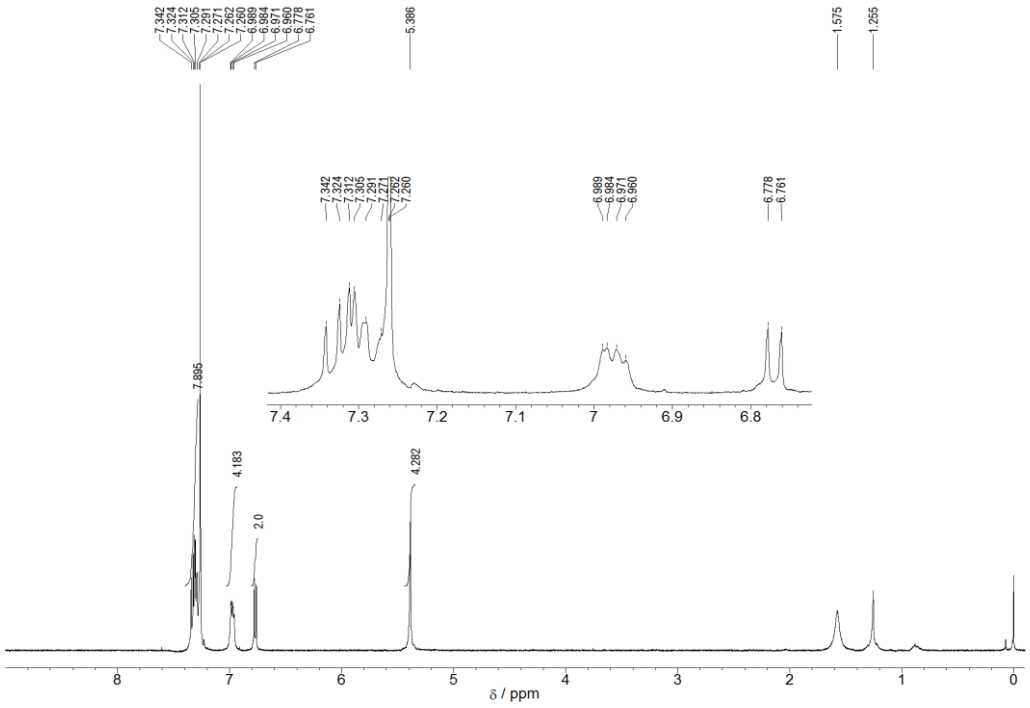

^{1}H NMR spectrum of **1c** in $CDCl_3$ solution (300 MHz).

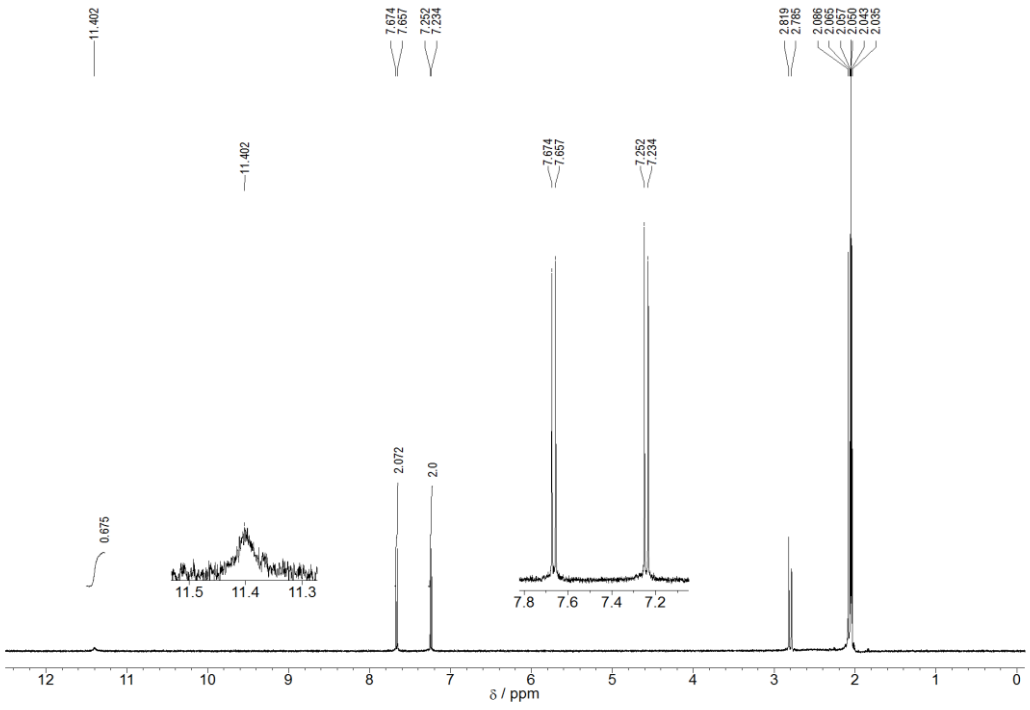

^{1}H NMR spectrum of **2a** in acetone-d_6 solution (300 MHz).

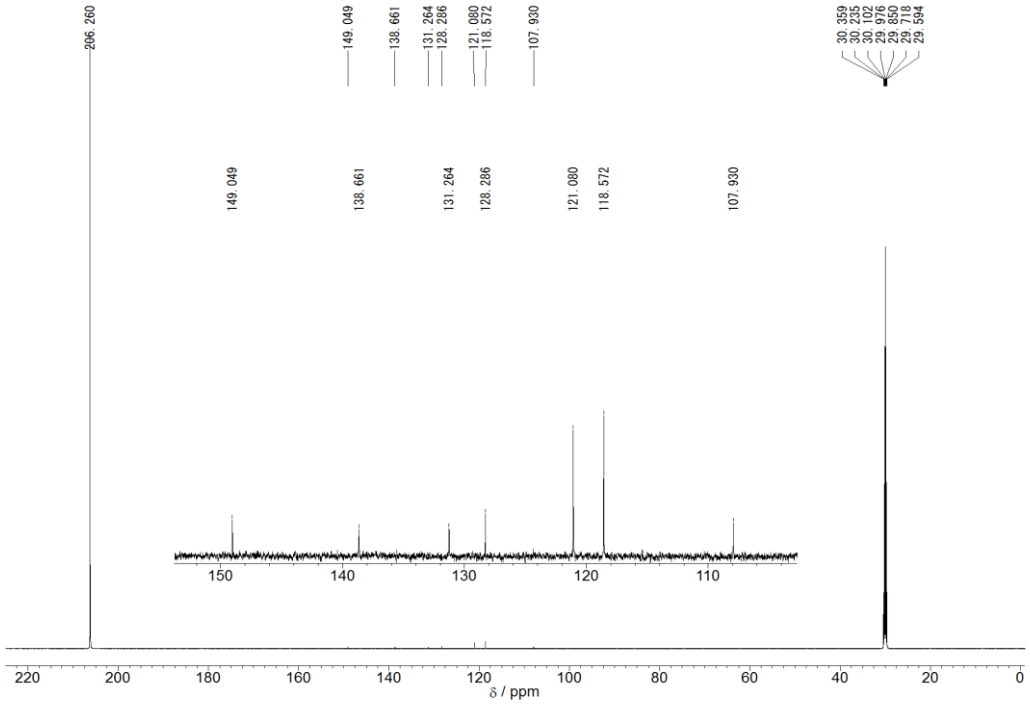

^{13}C NMR spectrum of **2a** in acetone-d_6 solution (150 MHz).

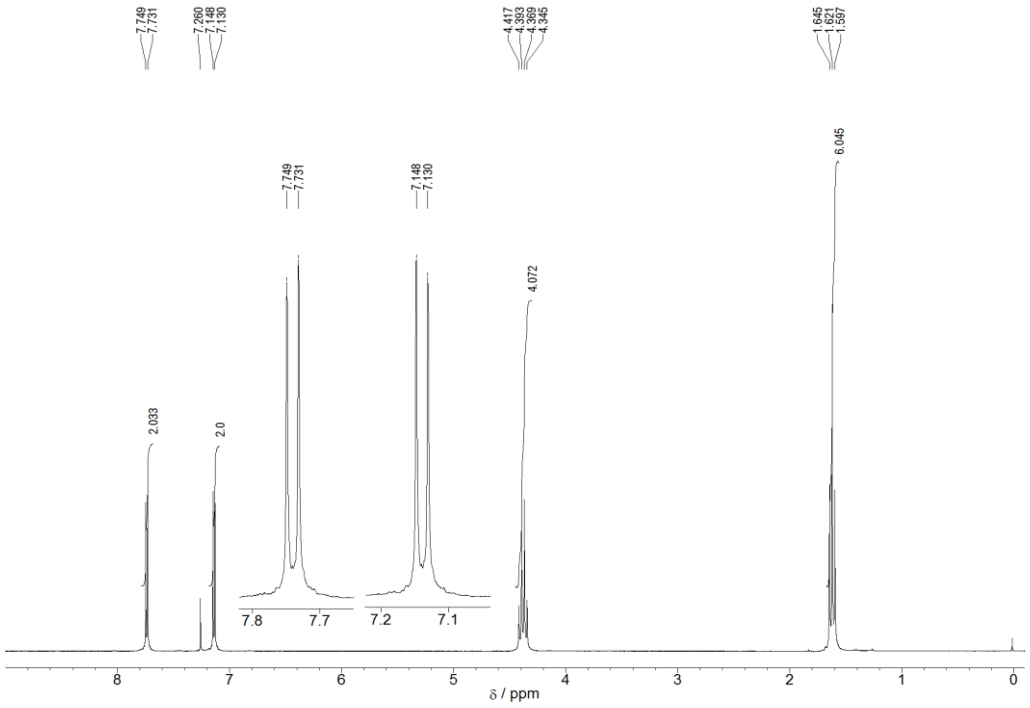

^{1}H NMR spectrum of **2b** in $CDCl_3$ solution (300 MHz).

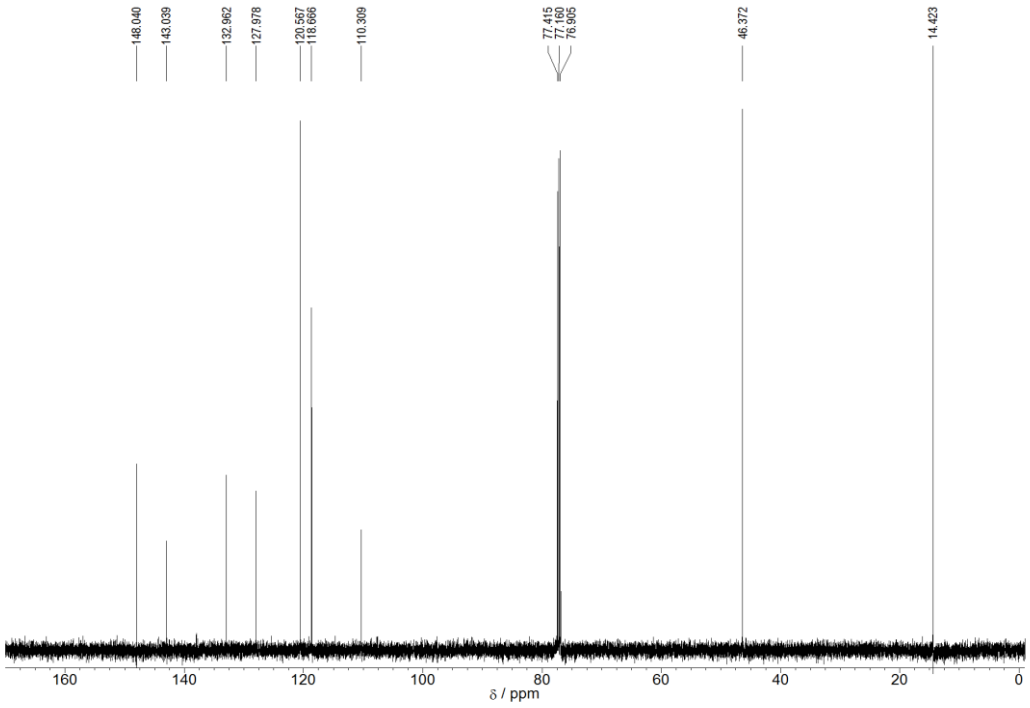

^{13}C NMR spectrum of **2b** in $CDCl_3$ solution (125 MHz).

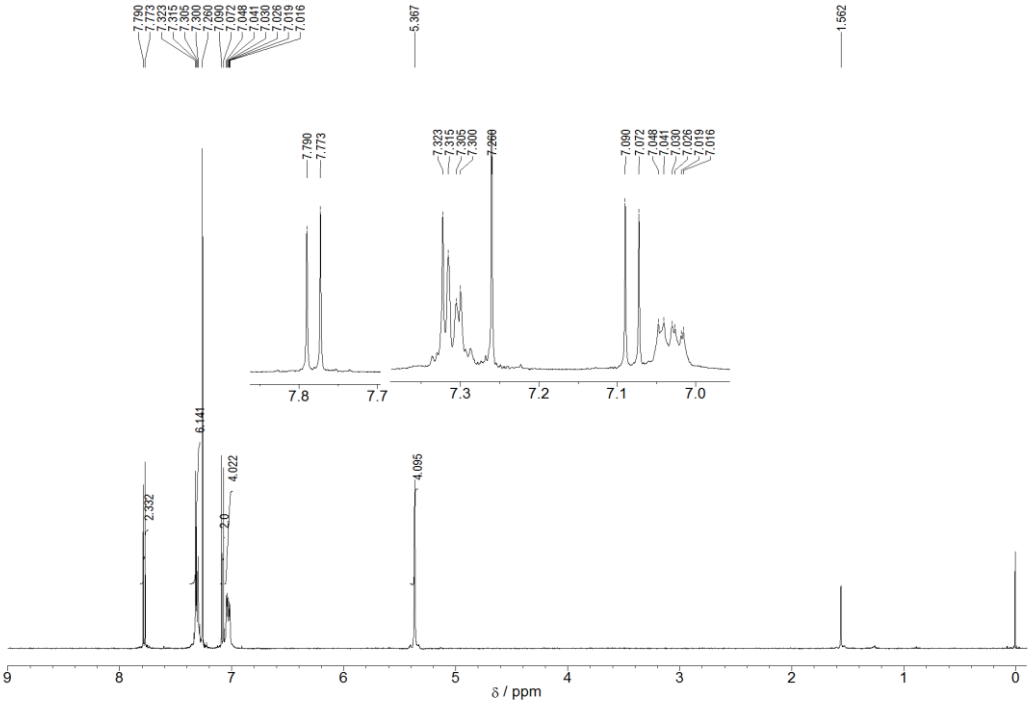

^{1}H NMR spectrum of **2c** in $CDCl_3$ solution (300 MHz).

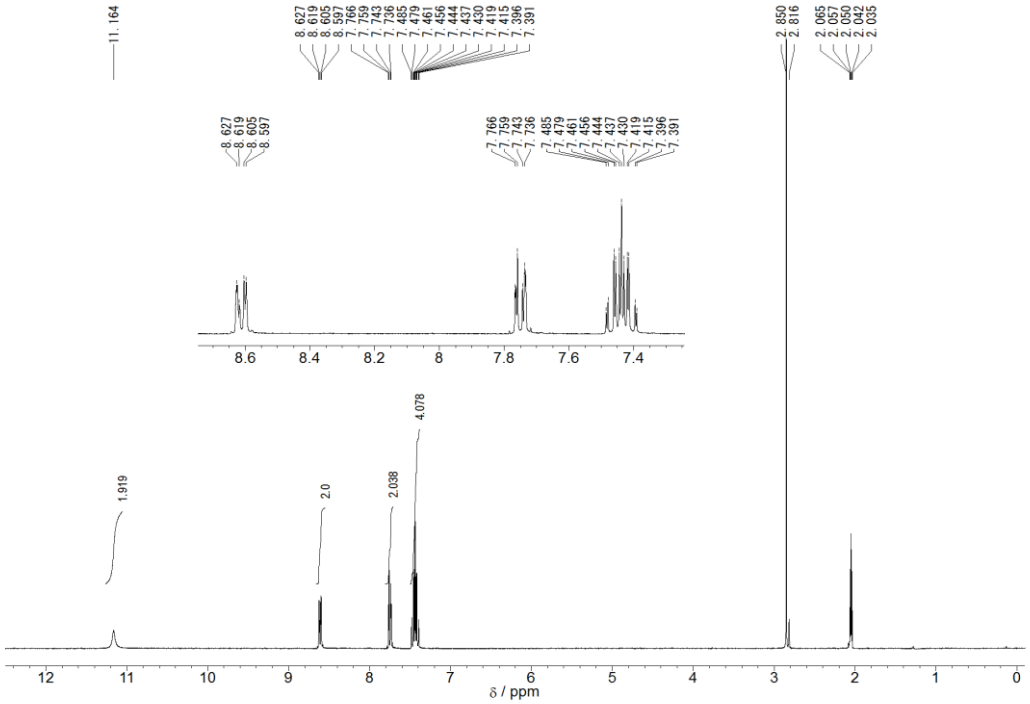

^{1}H NMR spectrum of **3a** in acetone-d_6 solution (300 MHz).

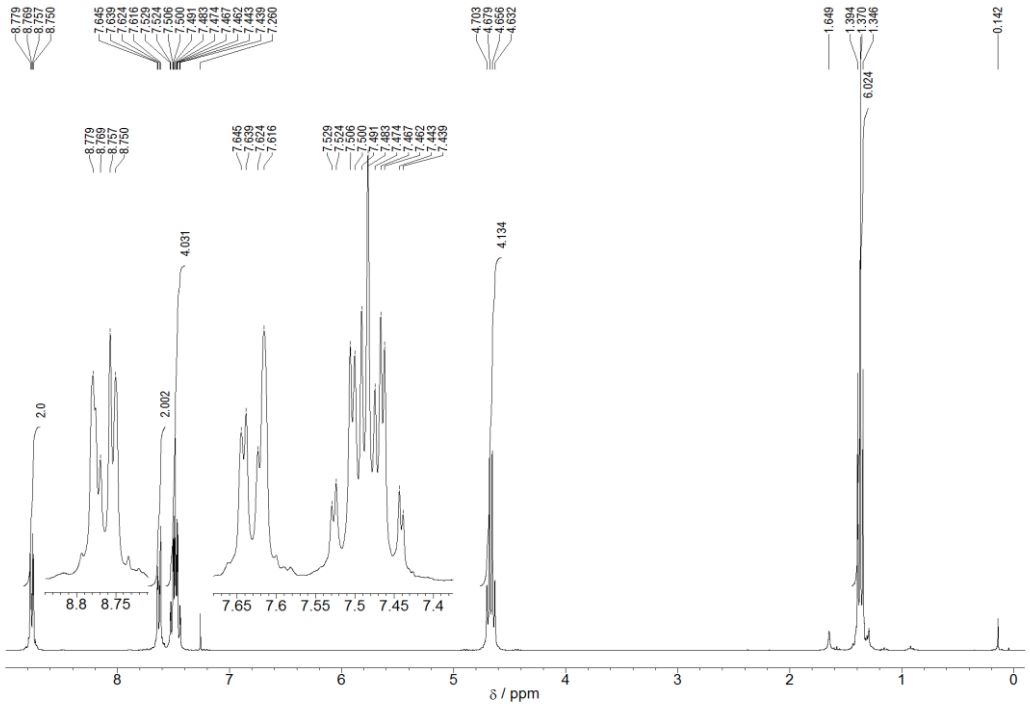

^{1}H NMR spectrum of **3b** in $CDCl_3$ solution (300 MHz).

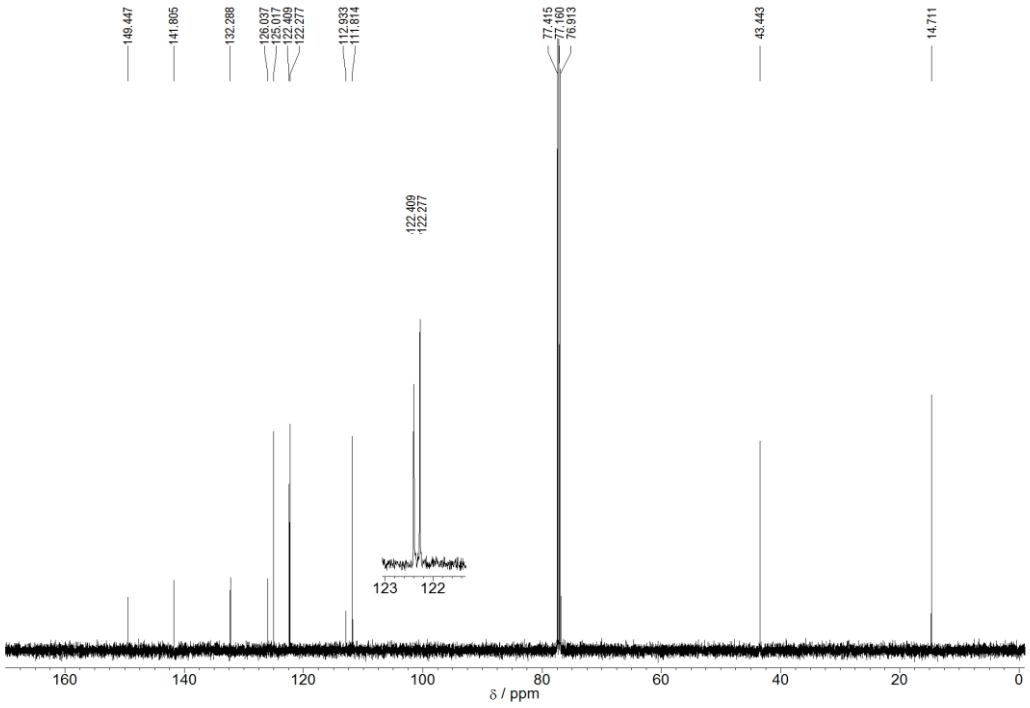

^{13}C NMR spectrum of **3b** in $CDCl_3$ solution (125 MHz).

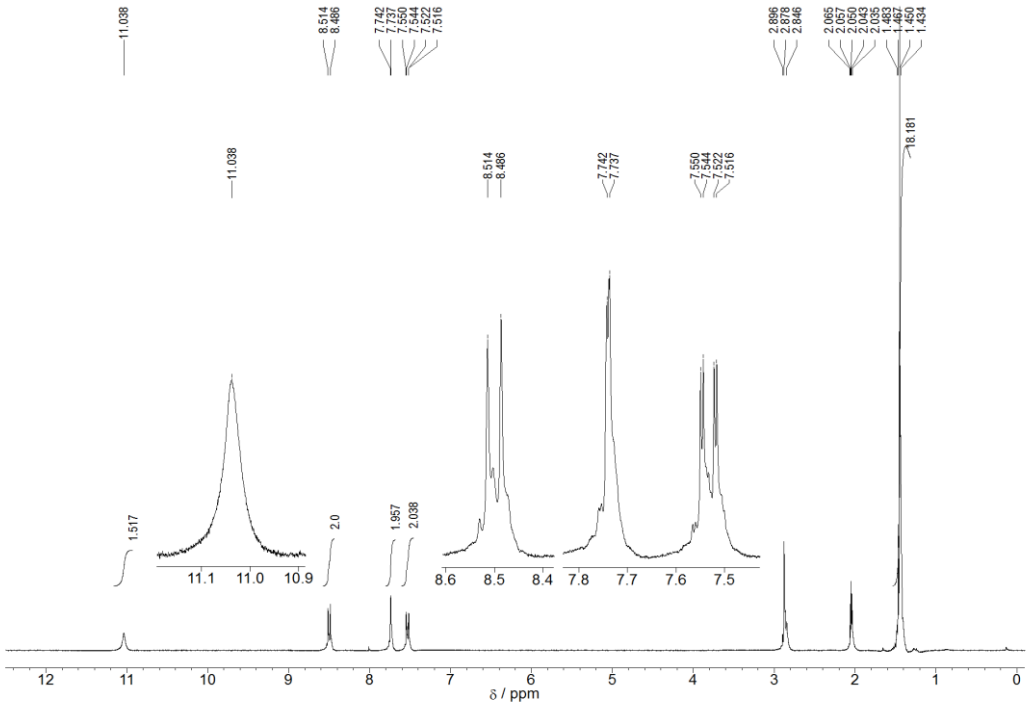

^{1}H NMR spectrum of **4a** in acetone-d_6 solution (300 MHz).

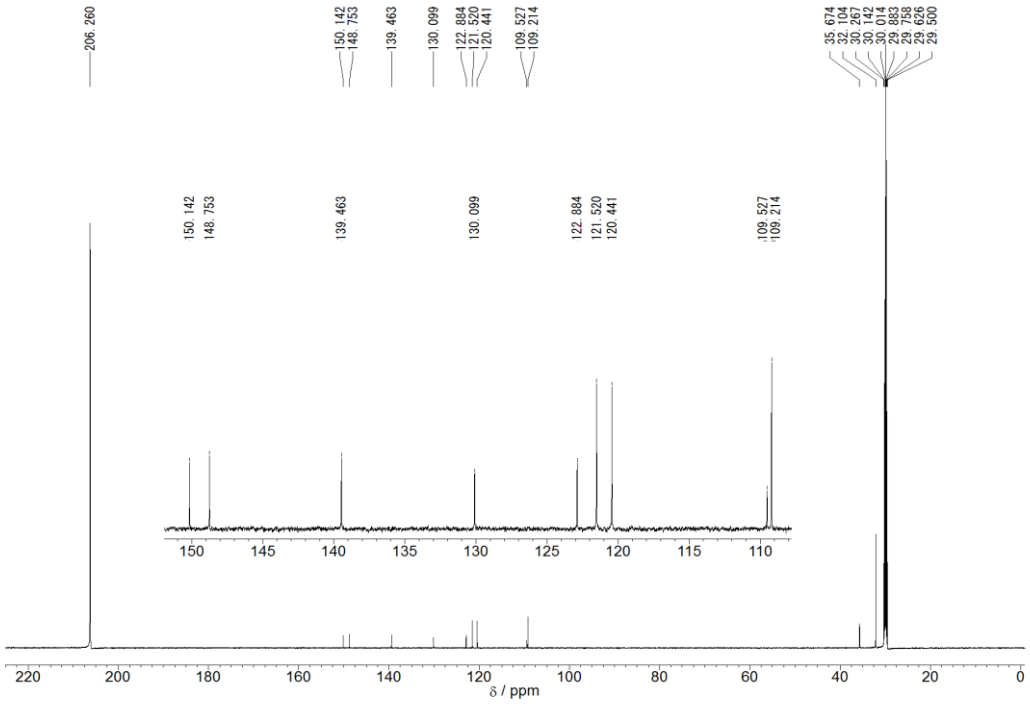

^{13}C NMR spectrum of **4a** in acetone-d_6 solution (150 MHz).

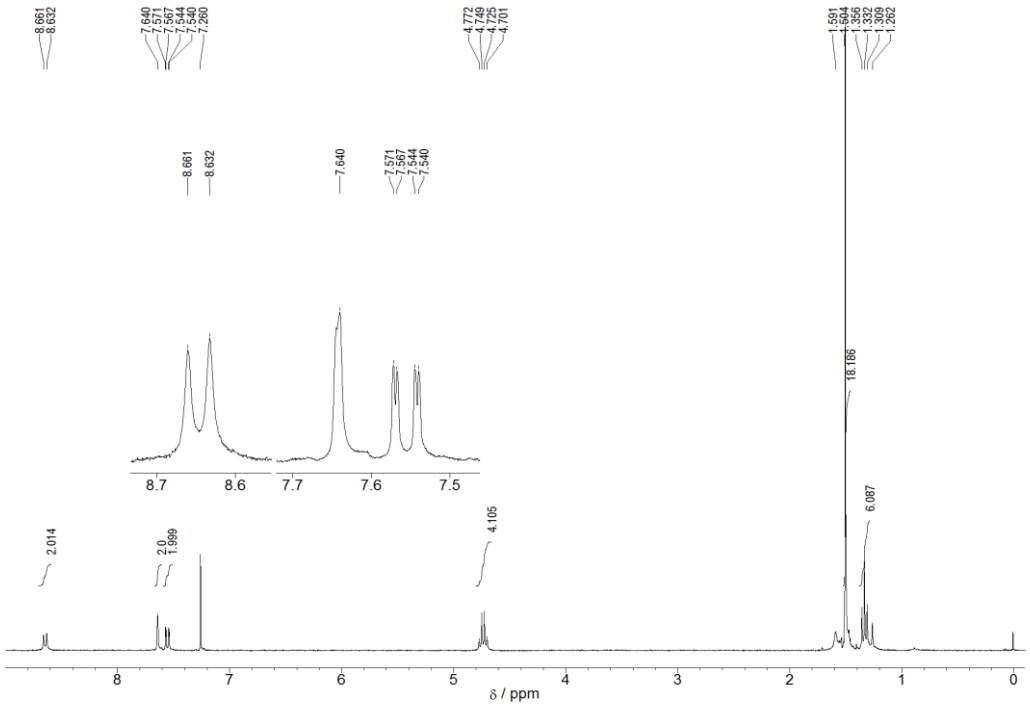

^{1}H NMR spectrum of **4b** in $CDCl_3$ solution (300 MHz).

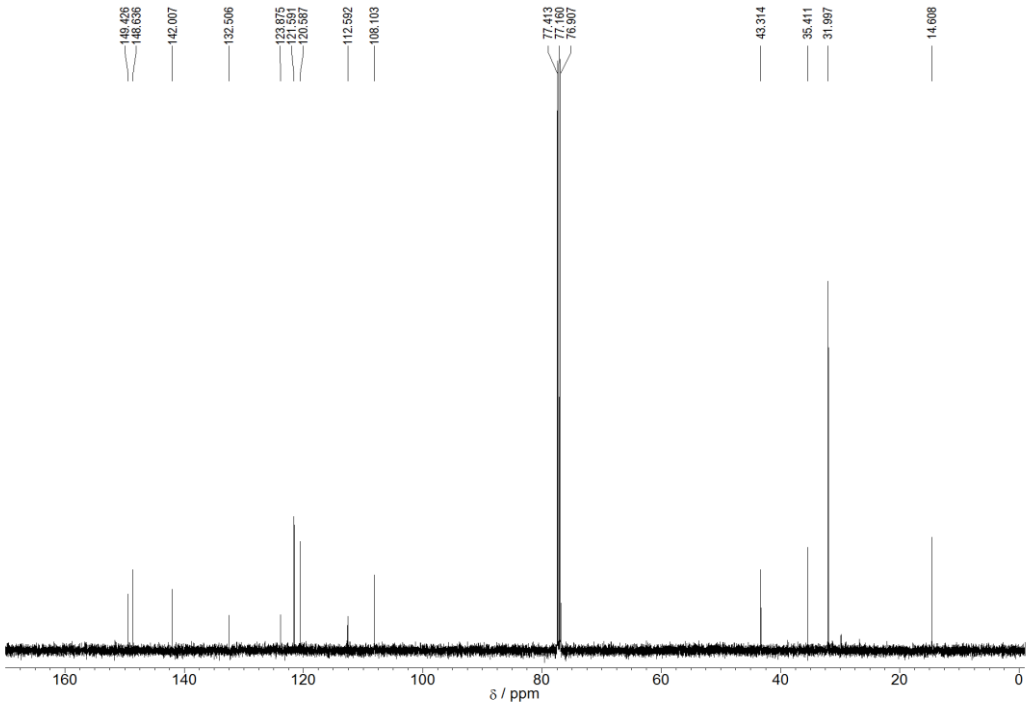

^{13}C NMR spectrum of **4b** in $CDCl_3$ solution (125 MHz).

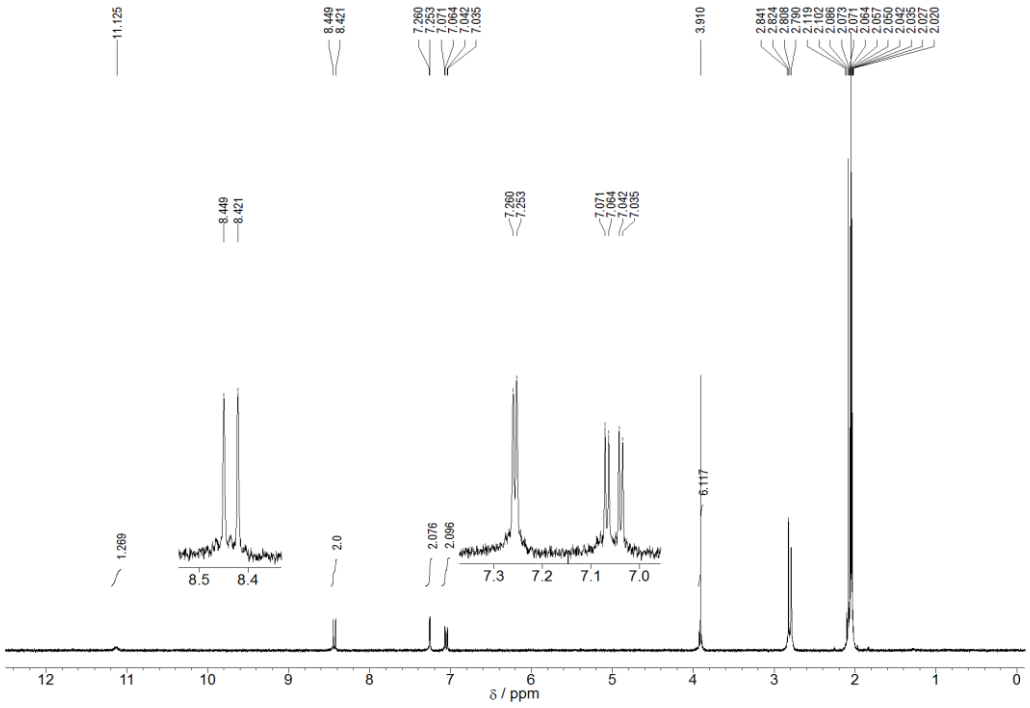

^{1}H NMR spectrum of **5a** in acetone-d_6 solution (300 MHz).

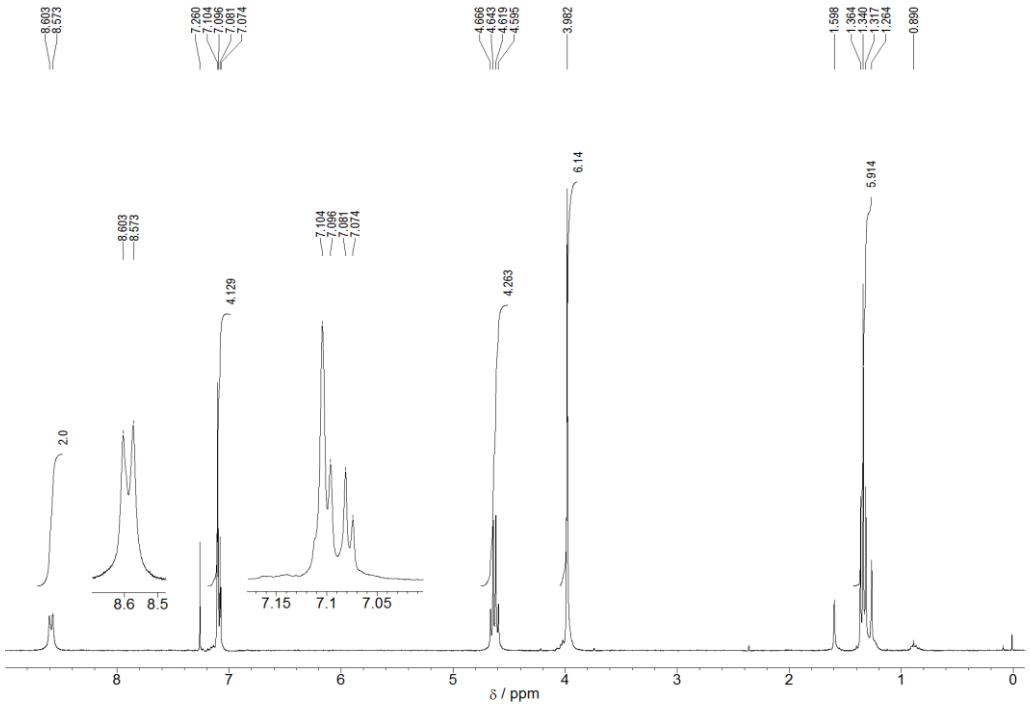

^{1}H NMR spectrum of **5b** in $CDCl_3$ solution (300 MHz).

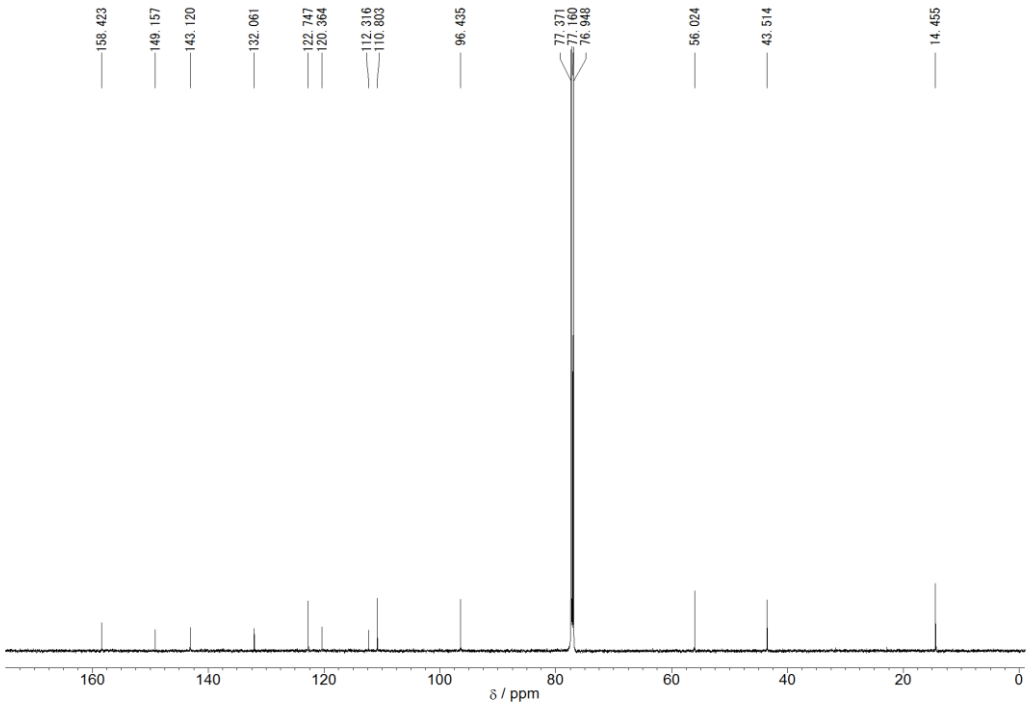

^{13}C NMR spectrum of **5b** in $CDCl_3$ solution (150 MHz).

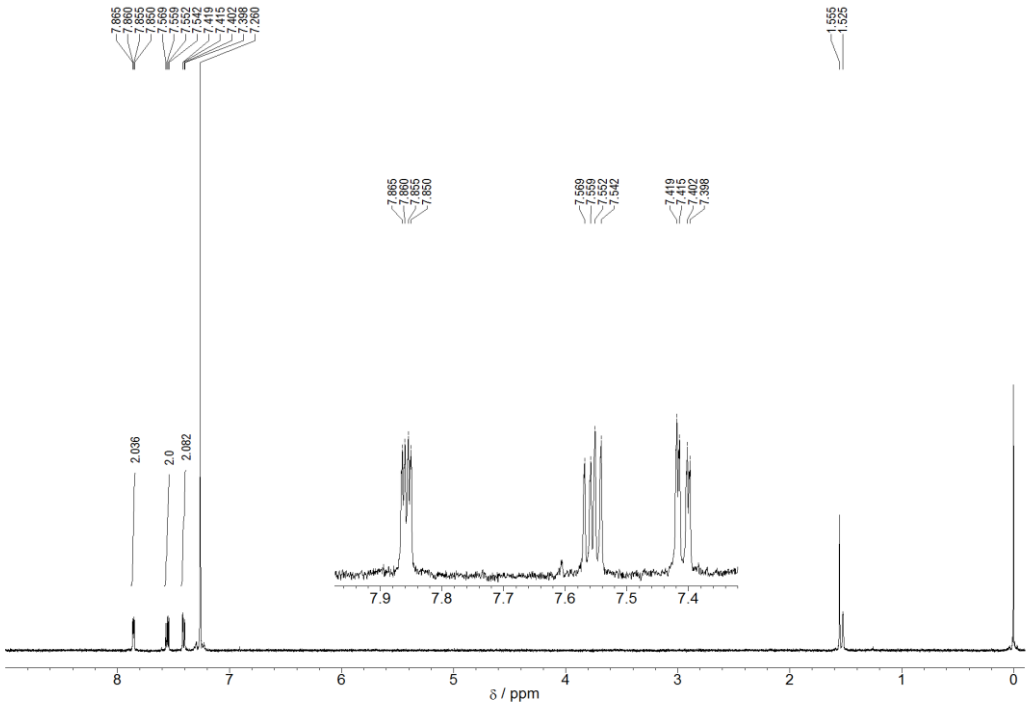

^{1}H NMR spectrum of **8** in $CDCl_3$ solution (300 MHz).

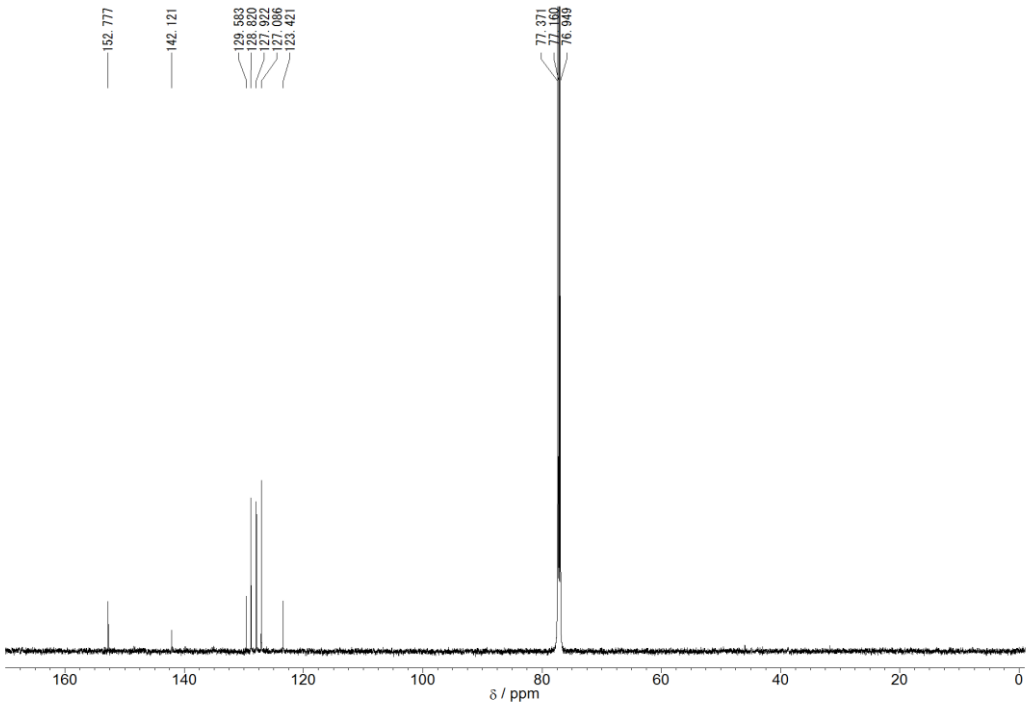

^{13}C NMR spectrum of **8** in $CDCl_3$ solution (150 MHz).

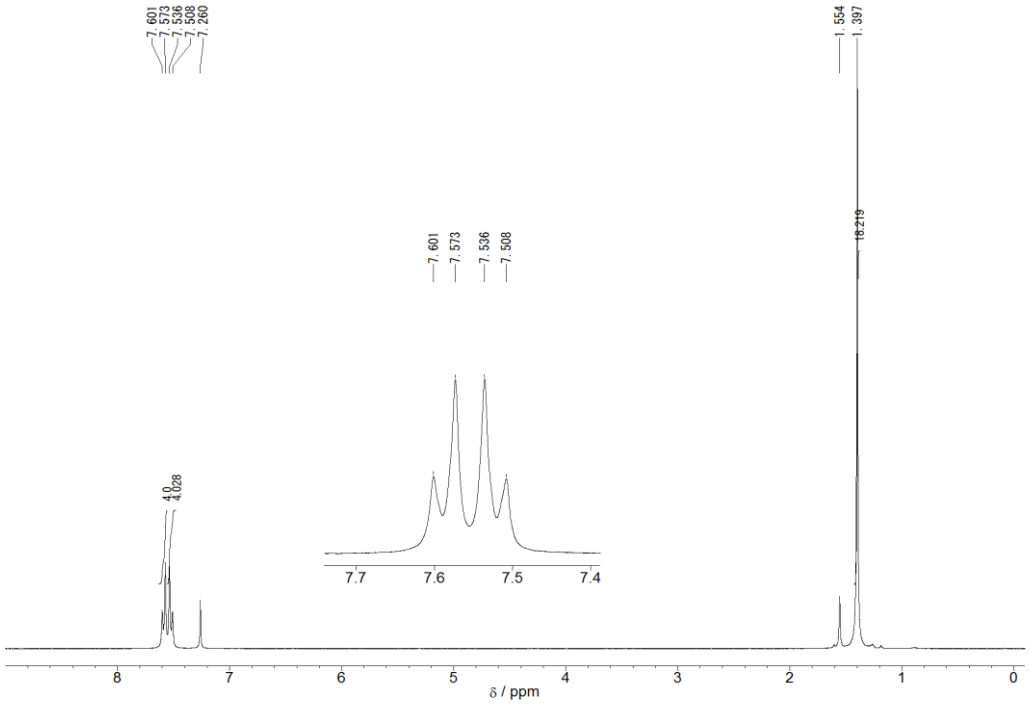

^{1}H NMR spectrum of **10** in $CDCl_3$ solution (400 MHz).

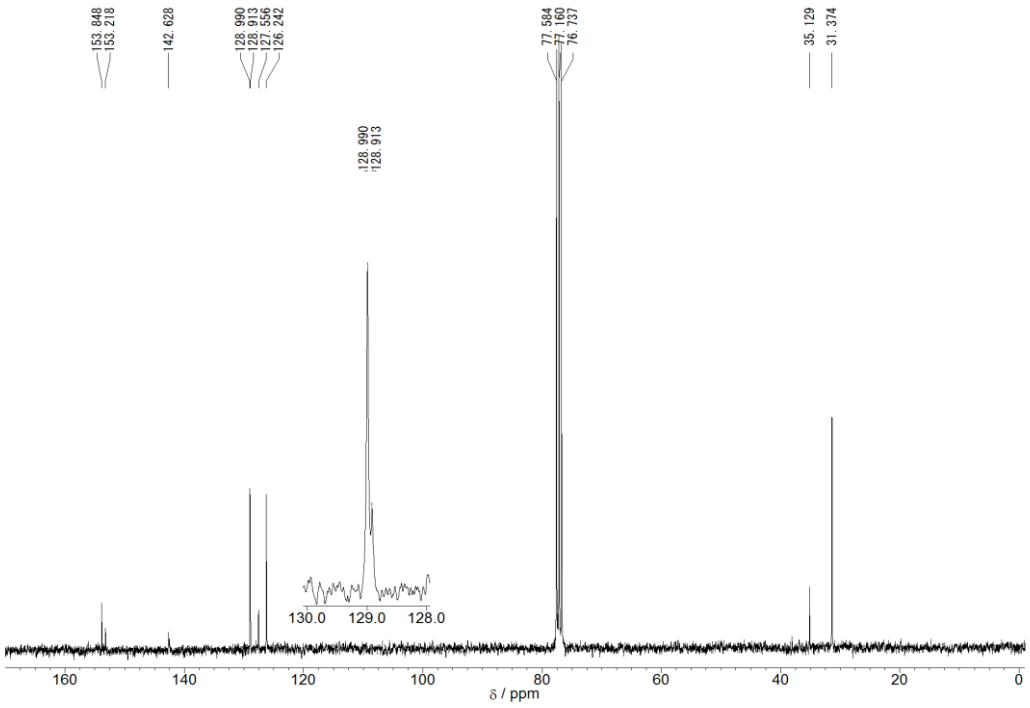

^{13}C NMR spectrum of **10** in $CDCl_3$ solution (75 MHz).

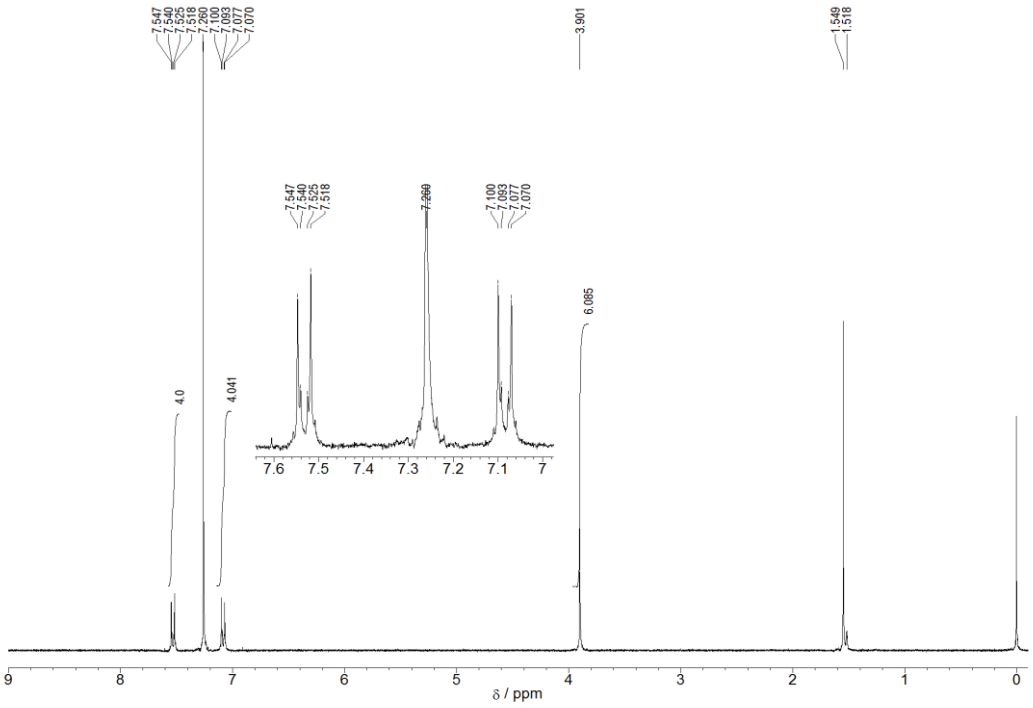

^{1}H NMR spectrum of **11** in $CDCl_3$ solution (300 MHz).

9. References

1. Uno, T.; Takagi, K.; Tomoeda, M. *Chem. Pharm. Bull.* **1980**, *28*, 1909.
2. Zoombelt, A. P.; Fonrodona, M.; Turbiez, M. G. R.; Wienk, M. M.; Janssen, R. A. J. *J. Mater. Chem.* **2009**, *19*, 5336.
3. Balaji, G.; Shim, W. L.; Parameswaran, M.; Valiyaveettil, S. *Org. Lett.* **2009**, *11*, 4450.
4. Frisch, M. J.; Trucks, G. W.; Schlegel, H. B.; Scuseria, G. E.; Robb, M. A.; Cheeseman, J. R.; Montgomery, J. A., Jr.; Vreven, T.; Kudin, K. N.; Burant, J. C.; Millam, J. M.; Iyengar, S. S.; Tomasi, J.; Barone, V.; Mennucci, B.; Cossi, M.; Scalmani, G.; Rega, N.; Petersson, G. A.; Nakatsuji, H.; Hada, M.; Ehara, M.; Toyota, K.; Fukuda, R.; Hasegawa, J.; Ishida, M.; Nakajima, T.; Honda, Y.; Kitao, O.; Nakai, H.; Klene, M.; Li, X.; Knox, J. E.; Hratchian, H. P.; Cross, J. B.; Bakken, V.; Adamo, C.; Jaramillo, J.; Gomperts, R.; Stratmann, R. E.; Yazyev, O.; Austin, A. J.; Cammi, R.; Pomelli, C.; Ochterski, J. W.; Ayala, P. Y.; Morokuma, K.; Voth, G. A.; Salvador, P.; Dannenberg, J. J.; Zakrzewski, V. G.; Dapprich, S.; Daniels, A. D.; Strain, M. C.; Farkas, O.; Malick, D. K.; Rabuck, A. D.; Raghavachari, K.; Foresman, J. B.; Ortiz, J. V.; Cui, Q.; Baboul, A. G.; Clifford, S.; Cioslowski, J.; Stefanov, B. B.; Liu, G.; Liashenko, A.; Piskorz, P.; Komaromi, I.; Martin, R. L.; Fox, D. J.; Keith, T.; Al-Laham, M. A.; Peng, C. Y.; Nanayakkara, A.; Challacombe, M.; Gill, P. M. W.; Johnson, B.; Chen, W.; Wong, M. W.; Gonzalez, C.; Pople, J. A. Gaussian 03, revision C.02; Gaussian, Inc.: Wallingford, CT, 2004.
5. (a) Becje, A. D. *J. Chem. Phys.* **1993**, *98*, 5648. (b) Lee, C.; Yang, W.; Parr, R. G. *Phys. Rev. B* **1988**, *37*, 785.
6. Binkley, J. S.; Pople, J. A.; Hehre, W. J. *J. Am. Chem. Soc.* **1980**, *102*, 939.
7. (a) Petersson, G. A.; Al-Laham, M. A. *J. Chem. Phys.* **1991**, *94*, 6081. (b) Petersson, G. A.; Bennett, A.; Tensfeldt, T. G.; Al-Laham, M. A.; Shirley, W. A.; Mangzaris, J. *J. Chem. Phys.* **1988**, *89*, 2193.
8. Altomare, A.; Burla, M. C.; Camalli, M.; Cascarano, G. L.; Giacovazzo, C.; Guagliardi, A.; Moliterni, A. G. G.; Polidori, G.; Spagna, R. *J. Appl. Crystallogr.* **1999**, *32*, 115.
9. Sheldrick, G. M. SHELXL-97, Program for the Refinement of Crystal Structures, University of Göttingen, Germany, **1997**.

10. Kobayashi, A.; Takehira, K.; Yoshihara, T.; Uchiyama, S.; Tobita, S. *Photochem. Photobiol. Sci.* **2012**, *11*, 1368–1376.
11. Cheng, Y.-S.; Chen, C.-H.; Ho, Y.-J.; Chang, S.-W.; Witek, H. A.; Hsu, C.-S. *Org. Lett.* **2011**, *13*, 5484.
12. Biniek, L.; Bulut, I.; Lévêque, P.; Heiser, T.; Leclerc, N. *Tetrahedron Lett.* **2011**, *52*, 1811.